UILU-ENG 84-3616

Report No. 116

ANALYSIS OF THE INTENSITY FLUCTUATIONS OF OPTICAL EMISSION LINES IN WELD ARC PLASMAS

by

H. Houshmand and C. S. Gardner

Department of Electrical and Computer Engineering

Supported by
Contract No. US Army CERL
DACA88-83-C-0003
DACA88-84-C-0003

A Report of the

MATERIALS ENGINEERING - MECHANICAL BEHAVIOR

College of Engineering, University of Illinois at Urbana-Champaign

December 1984

ACKNOWLEDGEMENTS

The authors would like to acknowledge F. Kearney, V. Hock, D. Blackmon, R. Weber and F. Kisters of the U. S. Army Construction Engineering Research Laboratory for their assistance in collecting weld arc spectral data. This work was supported by the U. S. Army Corps of Engineers under contracts DACA88-83-C-0003 and DACA88-84-C-0003.

TABLE OF CONTENTS

LIST OF FIGURES

Figure Page

LIST OF TABLES

1. INTRODUCTION

The Electro-Optic Systems Laboratory at the University of Illinois, in conjunction with the Construction Engineering Research Laboratory of the U.S. Army Corps of Engineers, has been involved in the development of a real-time weld quality monitoring system [1], [2]. By analyzing the optical radiation from the weld arc plasma, conditions leading to weld defects, such as hydrogen contamination and flux loss, can be detected during the welding process.

Many weld flaws originate from fluctuations in the primary welding parameters of voltage and current and from variations in arc chemistry. The changes in weld arc composition can be detected by observing spectral components of the optical radiation emitted by the weld plasma. In previous work, it was observed that the intensities of various emission lines fluctuated in response to changing welding conditions [3]. This report investigates the factors causing the optical intensity fluctuations and their relation to voltage and current variations.

To measure the optical intensity fluctuations, a high resolution monochromator was configured as a narrow-band optical filter. An optical fiber bundle guided light from the weld arc to the monochromator entrance slit. A phototransistor and amplifier were positioned at the exit slit to measure the intensity of the narrow-band light passed by the monochromator. The amplifier was interfaced to a high speed A/D converter and an LSI 11/23 computer. The temporal fluctuations of the optical signal were then analyzed by using fast Fourier transform (FFT) algorithms. The weld current and voltage were also sampled by the A/D converter and then analyzed. The dominant frequency components of each weld parameter were identified and correlated with frequency components of the other weld parameters. Further analysis was

done by choosing dominant spectral features of the frequency spectrum, then isolating and observing their behavior. The results indicate that monitoring certain temporal frequencies in optical emissions, voltage, and current could lead to detection of shield gas flow rate reduction. Previous work had shown that monitoring the intensity of Ar line emissions would allow detection of shield gas loss [1].

2. BACKGROUND AND THEORY

Incomplete gas coverage of the weld arc will create an unstable welding condition and cause porosity, formed by gas entrapment during solidification, in the welded joint. The loss of shield gas allows the ambient atmosphere to come in contact with the molten puddle, permitting the inclusion of gases from the atmosphere in the weld [4]. Porosity may occur in steel due to the reaction of sulphur in the base metal with hydrogen from the arc atmosphere. This reduces the strength of the welded joints leading to weld failure [5]. Shea and Gardner [6] showed that the hydrogen concentration in the shield gas can be monitored by analyzing the intensity of optical emissions from H and Ar atoms. Insufficient gas shielding can also cause an increase in the fluctuation of the arc current and voltage, as seen in Figure 1.

A stable arc is characterized by spray transfer of metal between the electrode and weld plate. Spray transfer occurs when fine droplets or particles of the molten electrode metal are transferred rapidly through the welding arc from the electrode to the puddle. The diameters of the droplets are smaller than the diameter of the electrode. This type of transfer is experienced when using Ar plus small amounts of O_2 as the shield gas mixture. The spray transfer occurs because the Ar shielding gas exhibits a pinch effect on the molten tip of the electrode wire. This pinch effect physically limits the size of the molten ball that can form on the end of the electrode wire; therefore, only small droplets of metal form [4]. A minimum current density is needed, in addition to proper shield gas coverage, to achieve spray transfer, as seen in Figure 2 [7].

When the shield gas flow rate is reduced, the electron conduction process takes over. The cathode jet originates from the work piece and actually

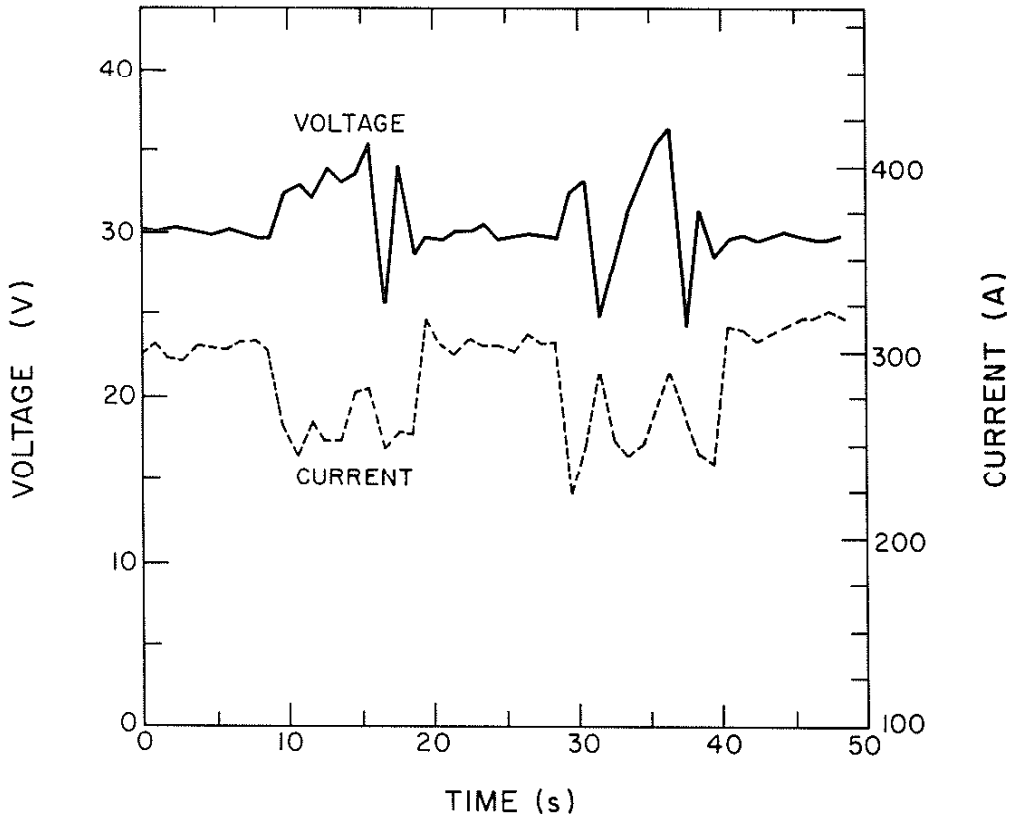

Figure 1. Variation of the arc voltage and current versus time. The Ar shielding gas was interrupted twice during this experiment for approximately ten seconds each time. The shielding gas was turned off at approximately 9 seconds and again at approximately 29 seconds [1].

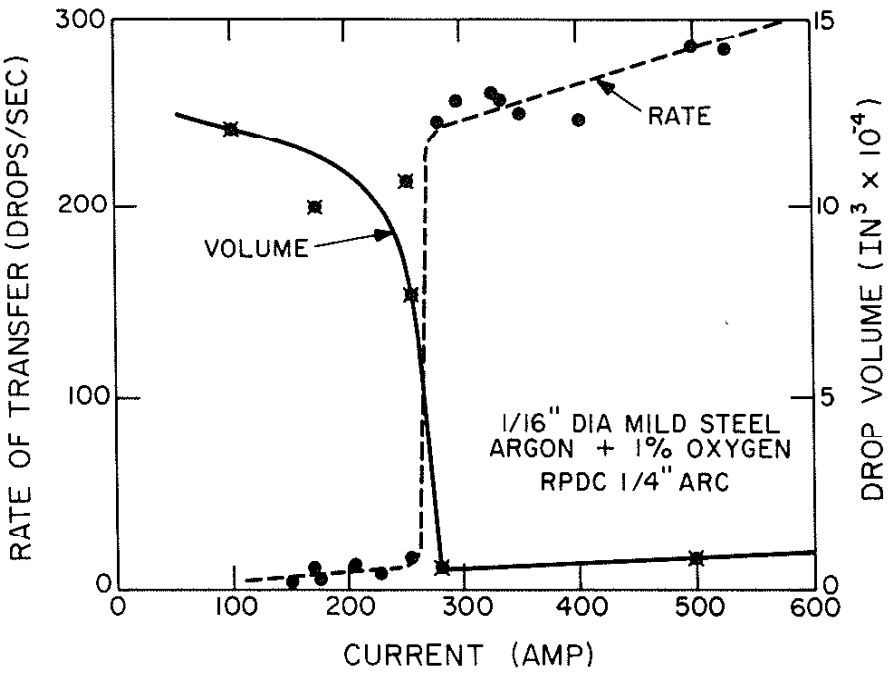

Figure 2. Effects of current on the size and frequency of drops transferred in an arc shielded by inert gas [7].

supports a ball on the tip of the electrode. When the molten ball grows to several times the size of the electrode diameter, it separates from the electrode and is transferred across the arc. As the globule is transferred across the arc, it is subjected to forces in the arc and takes on an irregular shape and a rotating motion, which causes the globule to reconnect with the electrode as well as with the work piece. This may cause a short circuit which momentarily extinguishes the arc. The globular transfer produces spatter which comes from both the molten puddle and the transfer metal.

Shortening of the arc and gas entrapment in the weld puddle, which changes the conductivity of the weld puddle, cause instability of current. The voltage becomes unstable for two reasons: the power supply counteracts the changes in current to provide a constant power output, and the formation of large globules at the tip of the electrode causes the arc length to change constantly [8]. Both the welding voltage and the welding current control the formation of the weld by influencing the depth of penetration, the bead width, and the bead height. They also affect deposition rate, arc stability, and spatter level [4].

In addition to monitoring the arc voltage and current, the intensity fluctuations of selected optical emission lines were measured during the experiments. The results are described in Chapter 5. In addition to the line spectra emitted by the excited atoms in the plasma, the hot arc and weld puddle emit a continuum radiation, which can be modeled as black-body radiation. A black body radiates electromagnetic energy whose distribution versus wavelength, $I(\lambda)$, is given by Planck's law [9]:

$$I(\lambda) = \frac{2\pi c^2 h}{\lambda^5 (e^{hc/\lambda KT} - 1)} \qquad (1)$$

where

λ = emitted radiation wavelength

h = Planck's constant = 6.6256×10^{-34} J-sec

K = Boltzmann's constant = 1.38054×10^{-23} J/K

c = speed of light = 2.997925×10^{8} m/sec

T = absolute temperature K.

As seen in Figure 3, the intensity of emitted light at a particular wavelength, λ_o, is temperature dependent.

The absolute intensity of radiation at a particular wavelength from arc weld plasma depends on the arc temperature, emissivity and the chemical composition of the arc. If self-absorption of radiation is neglected, the number of photons emitted from a small volume Δv corresponding to the transition between state m and state n is equal to $N_m A_{mn} \Delta v$, where A_{mn} is the transition probability from the state m to the state n and N_m is the number of particles per unit volume in the state m. Assuming local thermal equilibrium, N_m is related to the total number of particles, N, by the Boltzmann equation:

$$\frac{N_m}{N} = \frac{g_m e^{-E_m/KT}}{B(T)} \qquad (2)$$

where

E_m = energy of state m

g_m = degeneracy of state m

$B(T) = \sum g_r e^{-E_m/KT}$

r = all states .

Since the energy of a photon is $hv = E_m - E_n$, the radiation intensity per unit solid angle from volume element Δv is given by

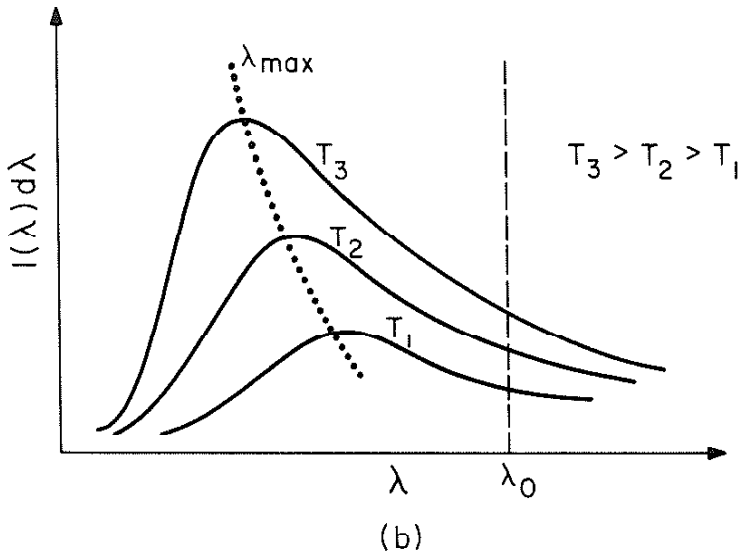

Figure 3. Black-body radiation [10].

$$I_{mn} = \frac{h\nu \, \Delta v \, N \, g_m \, A_{mn} \, e^{-E_m/KT}}{4\pi \, B(T)} \tag{3}$$

The absolute intensity at a particular wavelength is then found by integrating I_{mn} over all plasma volume elements Δv [11].

The temperature is needed to calculate the absolute intensity. Starting from Saha's equation, which relates the temperature to the ion density in the plasmas [11], it is possible to find a relationship between temperature, voltage gradient, and the current density. Assuming that the electron current density is much greater than the positive ion current density, which is justified by a much higher mobility of electrons compared to the positive ions, Saha's equation reduces to [12]

$$\log_{10} \frac{J^2}{E} = -5050 \frac{V_i}{T} + 1.5 \log_{10} T + 8.356 \tag{4}$$

where

V_i = the ionization potential of the gas

J = current density in A/cm^2 = weld current/plasma diameter

E = voltage gradient in V/cm = voltage across the arc/arc length

T = absolute temperature K.

Equations (1), (3), and (4) show that the electromagnetic radiation from the arc weld plasma is dependent upon current density and voltage gradient in a nonlinear fashion.

3. EXPERIMENTAL SETUP

The optical radiation from the weld arc is guided to the entrance slit of a monochromator, which serves as a tunable narrowband optical filter, by a lens and an optical fiber bundle mounted on the weld head. An optical detector mounted at the exit slit of the monochromator produces an analog electrical signal proportional to the light intensity passed by the monochromator. By using an A/D converter, the computer samples and stores this electrical signal. The system block diagram is depicted in Figure 4.

The base plate used in the experiments was ASTM-242 low alloy, high strength steel, and the welding electrode was E70S-3 solid wire. Table 1 lists the compositions of the base plate and electrode. A shield gas consisting of 98% Ar and 2% O_2 was used to isolate the arc plasma and molten weld pool from N_2, H_2 and other contaminating gases in air. The welder was an industrial grade, semi-automatic Gas Metal-Arc Welder.

The welding head was positioned on a motorized carriage, which had a 25 mm diameter lens with 50 mm focal length mounted on it. The lens, protected from welding spatter by a disk of pyrex glass, pointed at the arc and focused light from the weld arc onto a Dolan-Jenner, industrial-grade, armored optical fiber bundle [13]. The transmittance characteristics of the fiber versus wavelength are shown in Figure 5.

By using a 0.32 m Czerny-Turner type diffraction grating monochromator [14], the light was focused onto a 1200 line/mm holographic grating by a parabolic mirror. The grating disperses the light into its spectral components. A second mirror focused the spectrum onto the exit slit where a MFOD200 phototransistor optical detector, with the spectral response given in Figure 6, was positioned. The monochromator serves as a narrow-band optical filter focusing the light from a single emission line onto the detector.

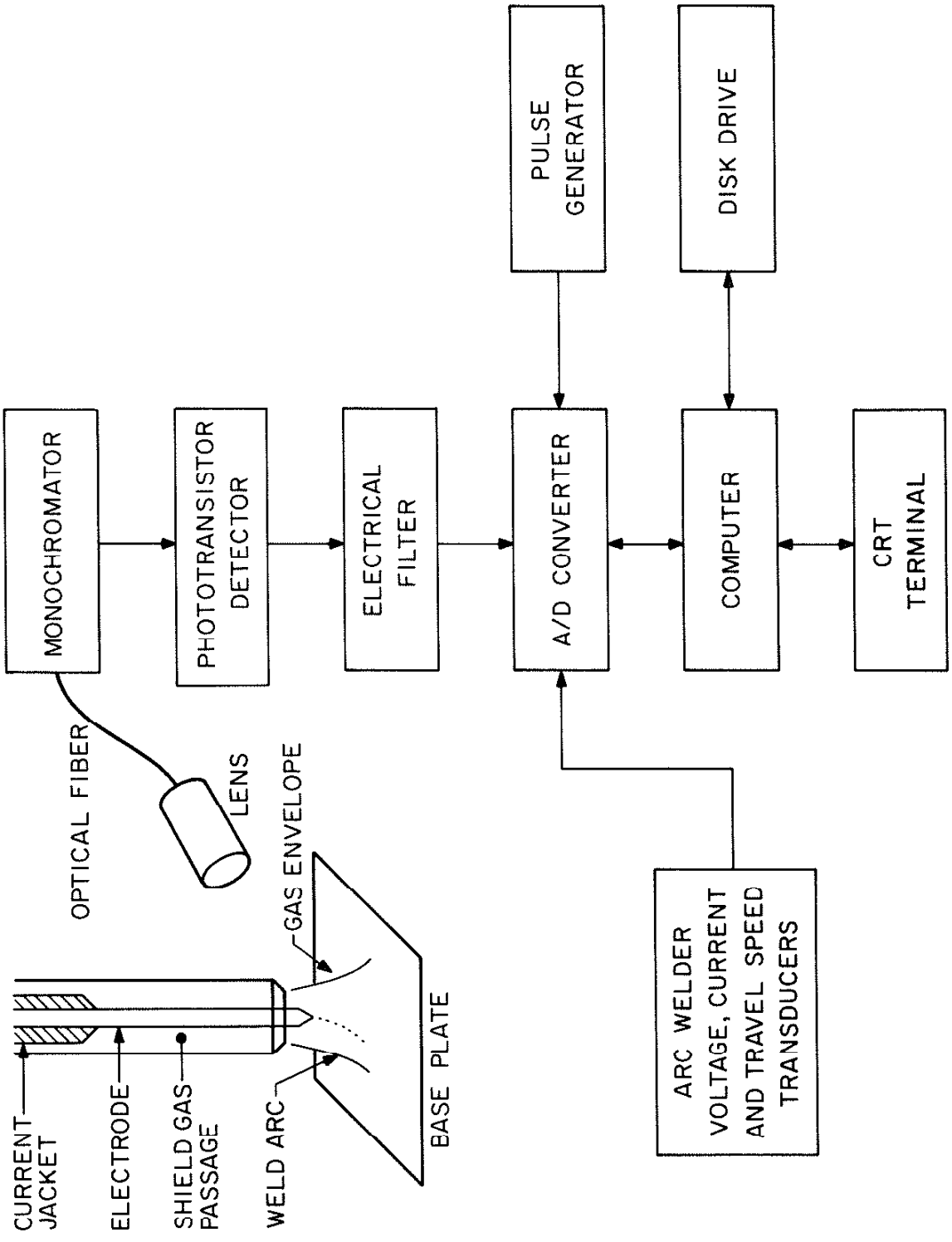

Figure 4. System block diagram.

TABLE 1

E70S-3 WELDING ELECTRODE COMPOSITION (%)

C	0.06-0.15
Mn	0.9-1.4
Si	0.45-0.70
P max	0.025
S max	0.035
Fe min	97.3

ASTM-242 LOW ALLOY STEEL COMPOSITION (%)

C	0.12
Mn	0.25-0.50
P	0.07-0.15
S	0.05 max
Si	0.25-0.55
Cu	0.25-0.40
Cr	0.4-0.65
V	0.02-0.10
Fe	Remainder

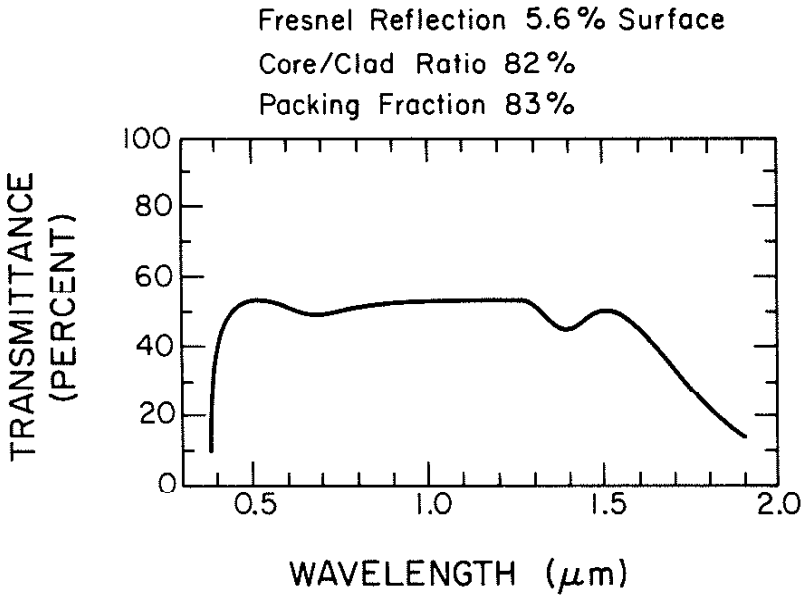

Figure 5. Optical fiber transmittance curve.

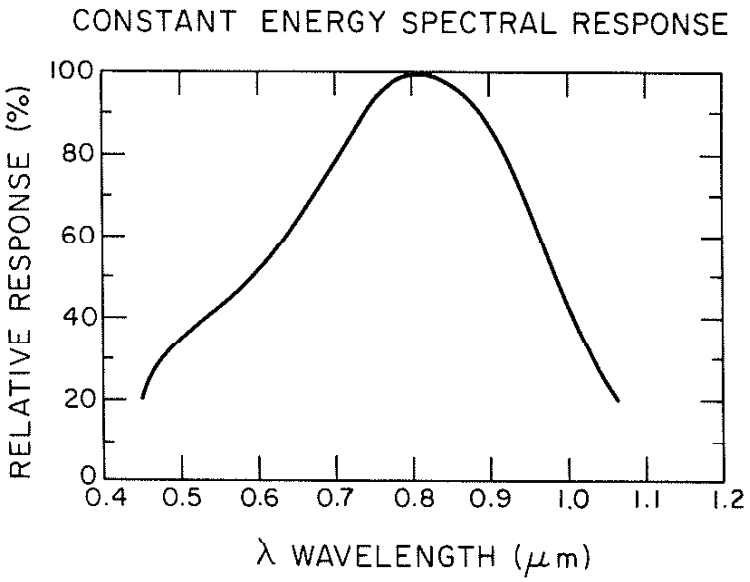

Figure 6. Spectral response of MFOD200 phototransistor.

The phototransistor produces current proportional to incident light intensity. A current-to-voltage converter circuit, followed by an amplifier, provides an electrical signal that is further processed by electrical filters. The electrical frequency response of the detector-amplifier combination is shown in Figure 7, and the circuit diagrams are given in Figure 8. The analog electrical filter reduces high frequency noise and band limits the signal. The filter output is then digitized, with a resolution of 4.88 mV under the control of a 16-bit LSI-11/23 microcomputer, by an ADAC model 1012 A/D converter [15] capable of taking up to 100,000 voltage samples per second.

The filter frequency response was chosen to satisfy the Nyquist sampling criterion, which states that, for complete signal recovery, the sampling rate should be twice the highest frequency component in the signal. The data sets were obtained by sampling at 20 kHz and 3 kHz. The signal sampled at 3 kHz was band limited by using a single pole RC filter with corner frequency of 250 Hz.

For each data set, 4096 voltage samples were taken and stored on a floppy disk, under the control of data acquisition software documented in Appendix A. The number of data sets taken is optional. For all the data reported here, the welder was adjusted for a current of 300 A at 30 V. The travel speed was 15 cm/min. The gas mixture was adjusted for 98% Ar and 2% O_2.

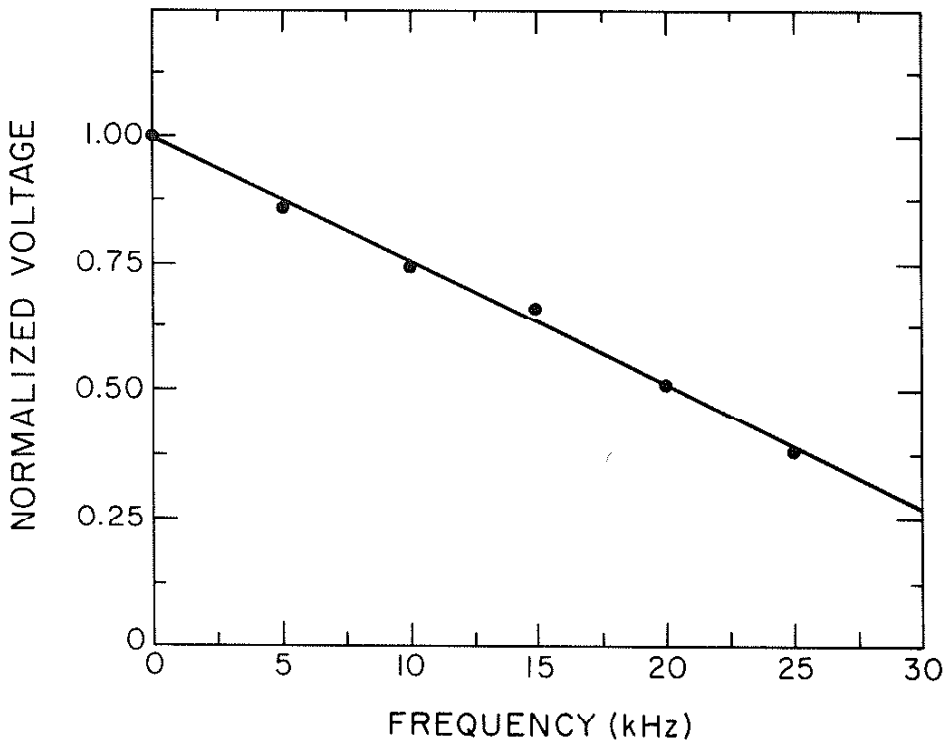

Figure 7. Electrical frequency response of the detector-amplifier combination.

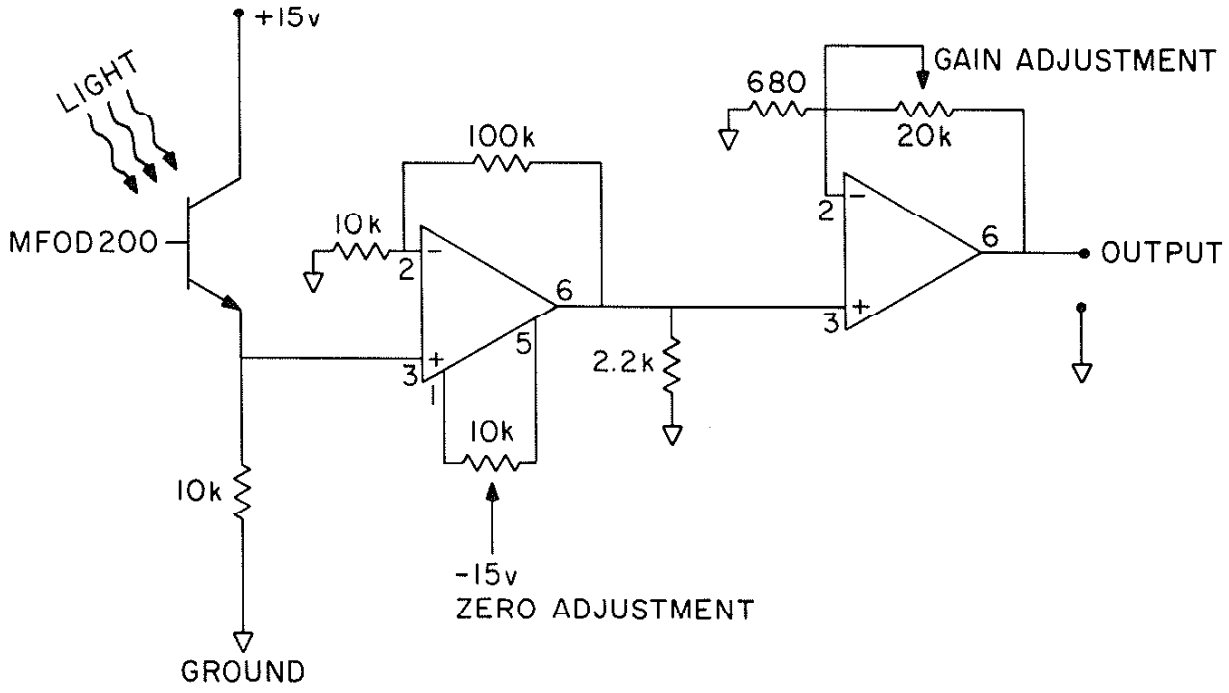

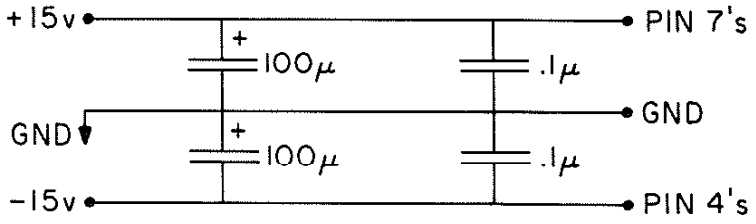

Figure 8. Detector-amplifier circuit diagram.

4. SIGNAL PROCESSING

During optimum metal transfer in Gas Metal-Arc Welding, the weld plasma is essentially uniform and the emitted radiation intensity is approximately constant. When the shield gas flow rate is reduced, the metal transfer becomes globular, and rapid changes in composition of weld plasma and instability of arc current cause the fluctuations of emitted light to increase. The intensity fluctuations of optical radiation emitted by Fe atoms at a wavelength of 4383.544 Å under optimum welding conditions and reduced shield gas flow rate are shown in Figure 9. A quasi-periodic signal with a period of about 4 msec is noticed in optimum welding data; the data of the reduced shield gas flow rate exhibit a similar fluctuation pattern in addition to a slower varying signal with a period on the order of 20 msec.

The exact period of these signals could be obtained by computing the Fourier transform of the weld data. More than one set of data was taken for each experimental condition. The frequency spectrum of each data set was obtained; then all of the power spectra [16] were averaged together. The mathematical relationship for the averaged power spectrum may be expressed as

$$\overline{S}(f) = \frac{1}{N} \sum_{i=1}^{N} S_i(f) \qquad (5)$$

where

i = the data set index number

N = total number of data sets

$S_i(f)$ = power spectrum of data set i.

This is illustrated in Figure 10. Figure 10a is the power spectrum of a single data set obtained under optimum welding conditions. Figure 10b is the average power spectrum obtained by averaging the power spectra from 10 data

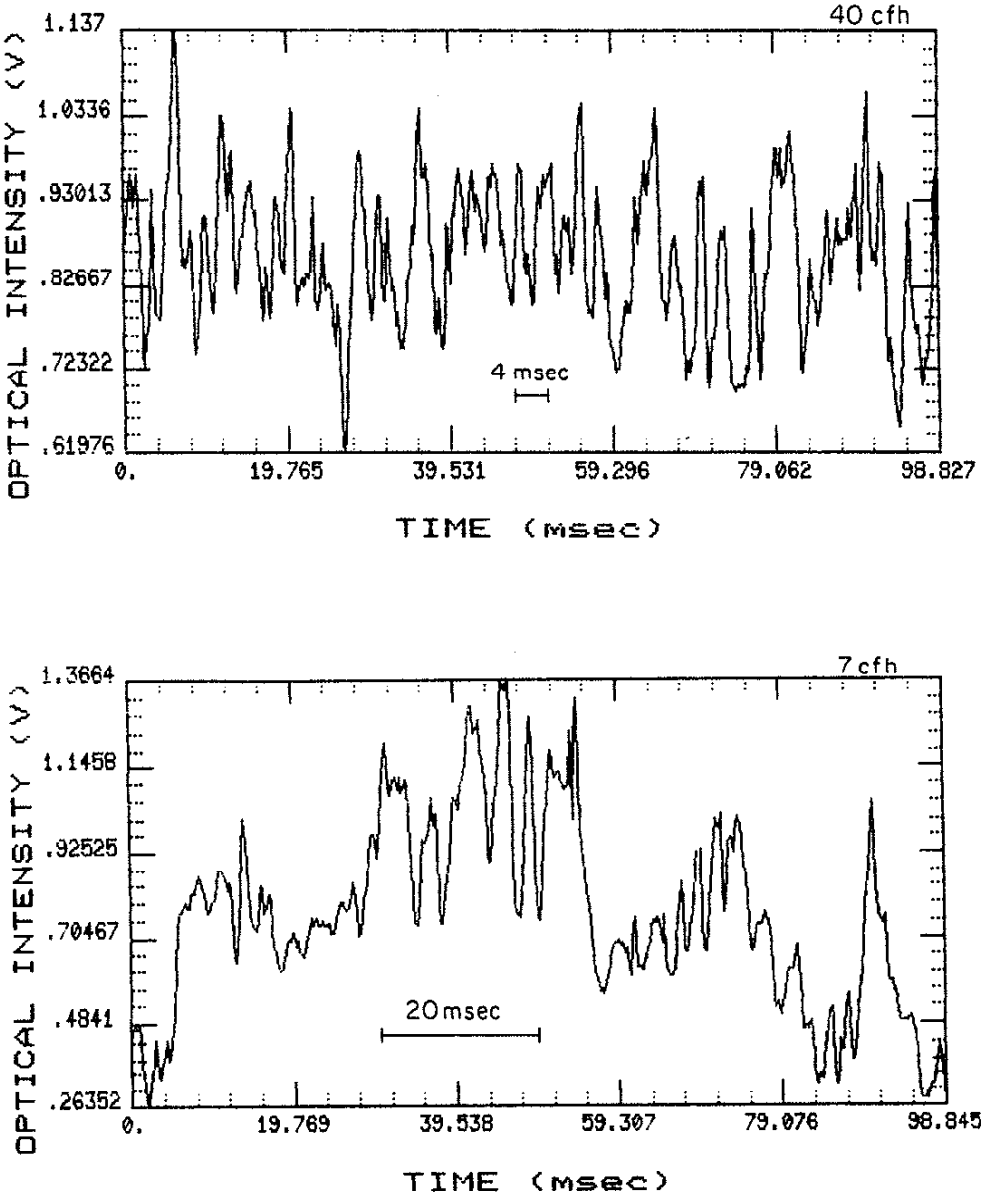

Figure 9. Optical intensity fluctuations of emissions by Fe atoms at 4383.544 Å. (a) Optimum welding, the Ar shield gas flow rate was 40 cfh. (b) The Ar shield gas flow rate was reduced to 7 cfh resulting in porosity.

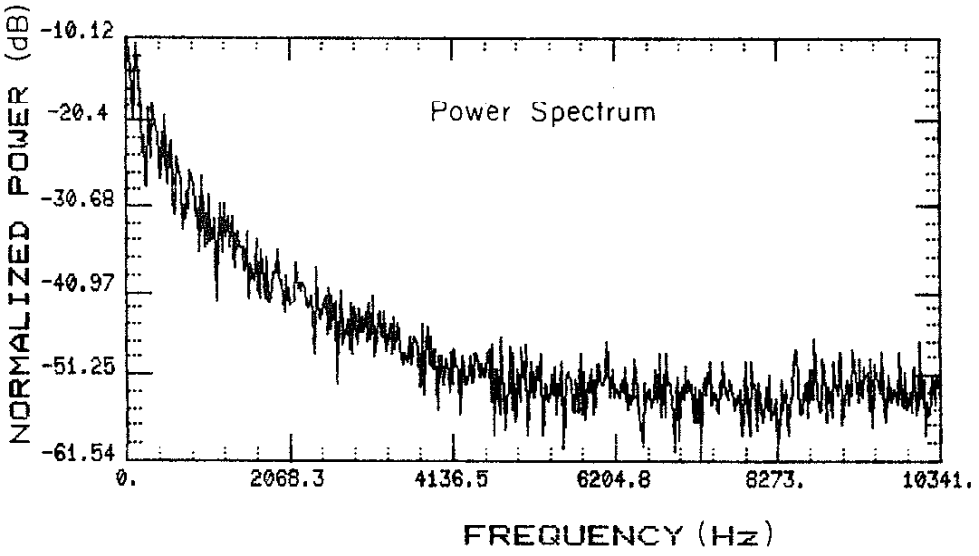

(a)

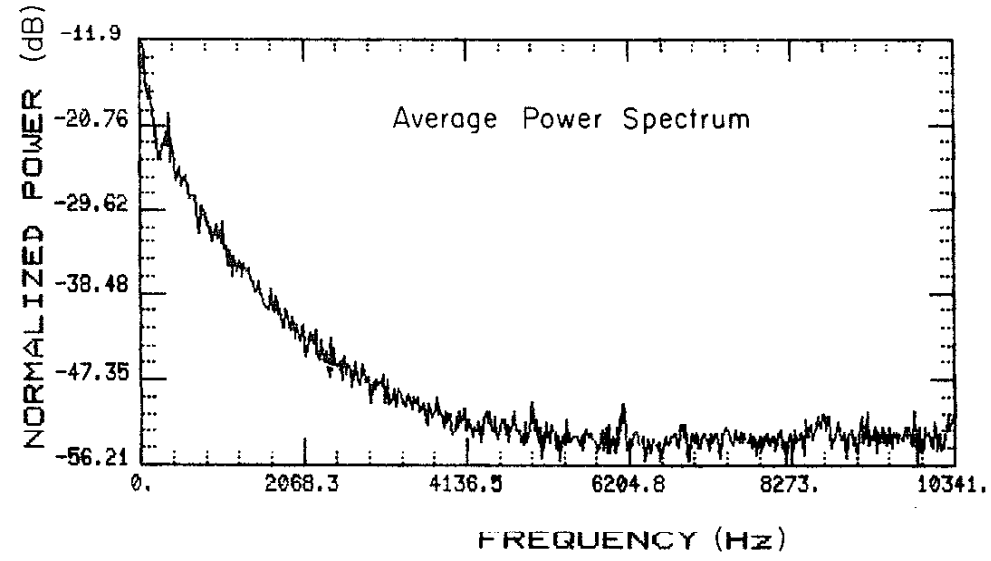

(b)

Figure 10. Power spectra of the intensity fluctuations of the 4383.544 Å Fe emission line under optimum welding conditions. (a) Power spectrum of a single data set. (b) Averaged power spectra of 10 data sets.

sets. Averaging reduces noise and enhances the dominant frequency components of the signal [17].

To eliminate the effects of gross variations in the intensity levels of the optical signals, the average power spectrum was normalized with respect to the total energy.

$$\overline{S}_N(f) = \frac{\overline{S}(f)\ \Delta f}{\int_{-\infty}^{\infty} df\ \overline{S}(f)} \tag{6}$$

where

$\Delta f = 1$ Hz.

A standard discrete Fourier transform technique was used to transform the time domain weld data to the frequency domain [18]. The computer programs are documented in Appendix B.

5. EXPERIMENTAL RESULTS

5.1. Arc Current

The arc current fluctuations in optimum Gas Metal-Arc Welding are shown in Figure 11a. The mean of these arc current fluctuations was 328.4 A. The fluctuations were relatively small in optimum welding, as indicated by a normalized standard deviation ($\sigma_I/\overline{I}$) of 0.0081. When the shield gas flow rate was reduced from the optimum level of 40 cfh to 18 cfh, the arc current mean reduced to 321.73 A. A major change in the arc current fluctuations was noticed when the shield gas flow rate was further reduced to 7 cfh, the current mean dropped to 272.17 A and the standard deviation rose to 42.55 A. Both the reduction in Ar shield gas flow rate, which reduced the spray transfer, and the drop in the current below the threshold required for spray transfer contributed to the increase in current fluctuations. The current mean, tabulated in Figure 12, dropped as the shield gas flow rate was reduced, which could have been caused by the arc channel density reduction, reducing the channel conductivity.

The welder power supply full-wave rectified a three-phase AC input. Therefore, the welding current was expected to contain a small 60 Hz component and harmonics of 60 Hz. Figure 13a displays the power spectra of the arc current fluctuations; 60 Hz and its harmonics are the distinguishable frequency components. The frequency component 60.34 Hz corresponds to a period of 16.57 msec--the quasi-periodic signal in arc current fluctuations (see Figure 11a) had a period of about 16 msec.

As the shield gas flow rate was reduced, the power below 40 Hz increased, but the power of the signal centered at 60 Hz decreased. The ratio of the power in these frequency ranges could provide a number that could be sensitive

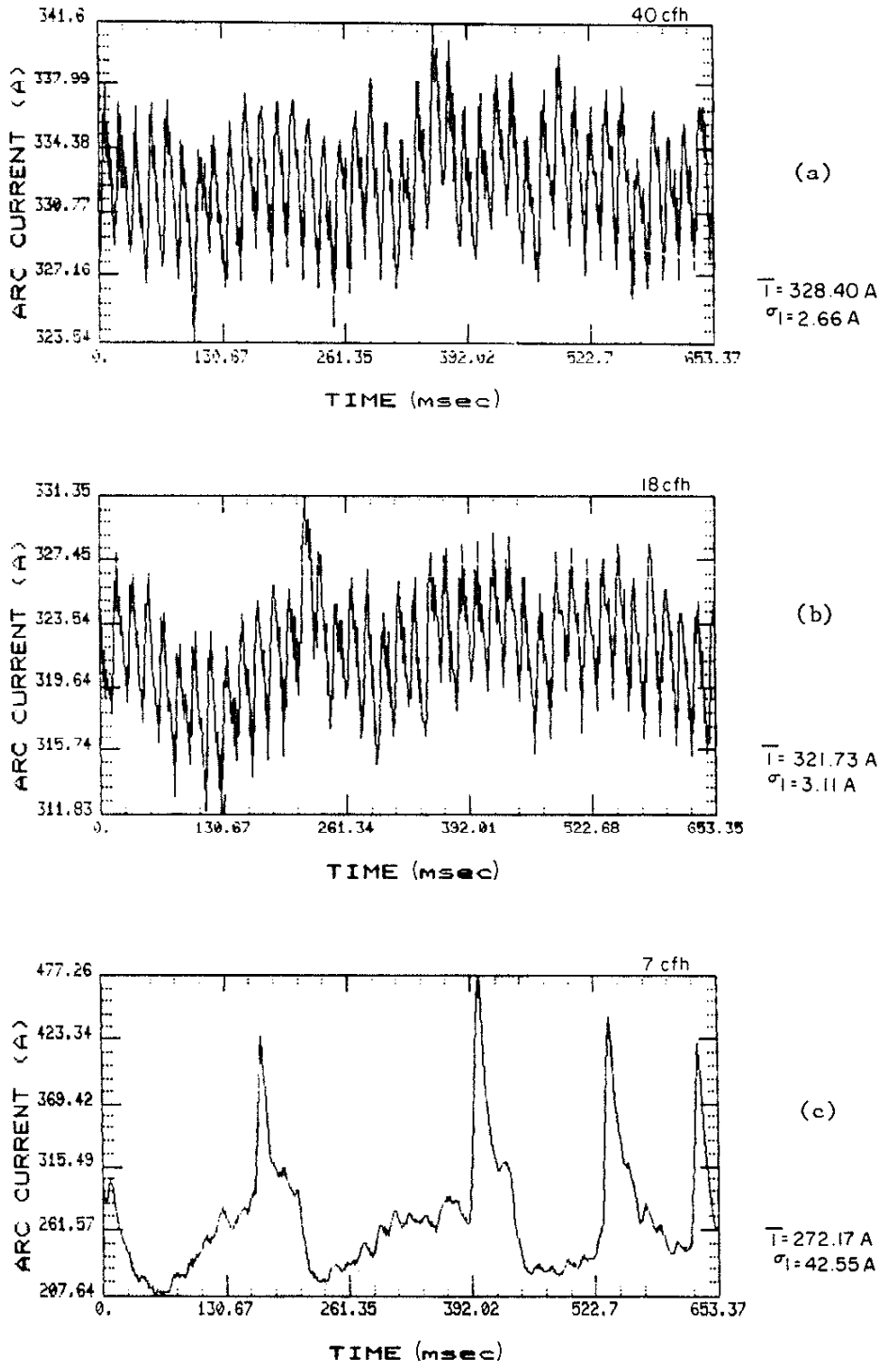

Figure 11. Current fluctuations sampled at 3.1284 kHz. (a) Optimum welding, shield gas flow rate was 40 cfh. (b) Shield gas flow rate was 18 cfh. (c) Shield gas flow rate was 7 cfh.

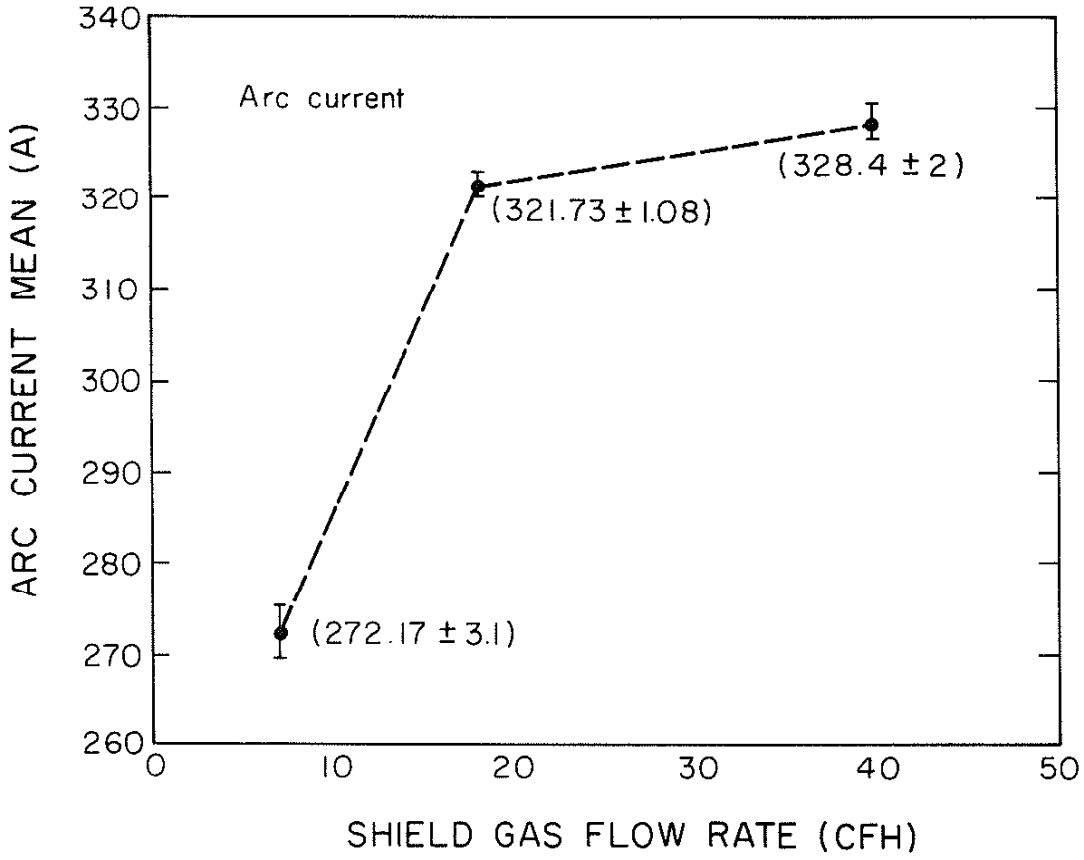

Figure 12. Arc current mean.

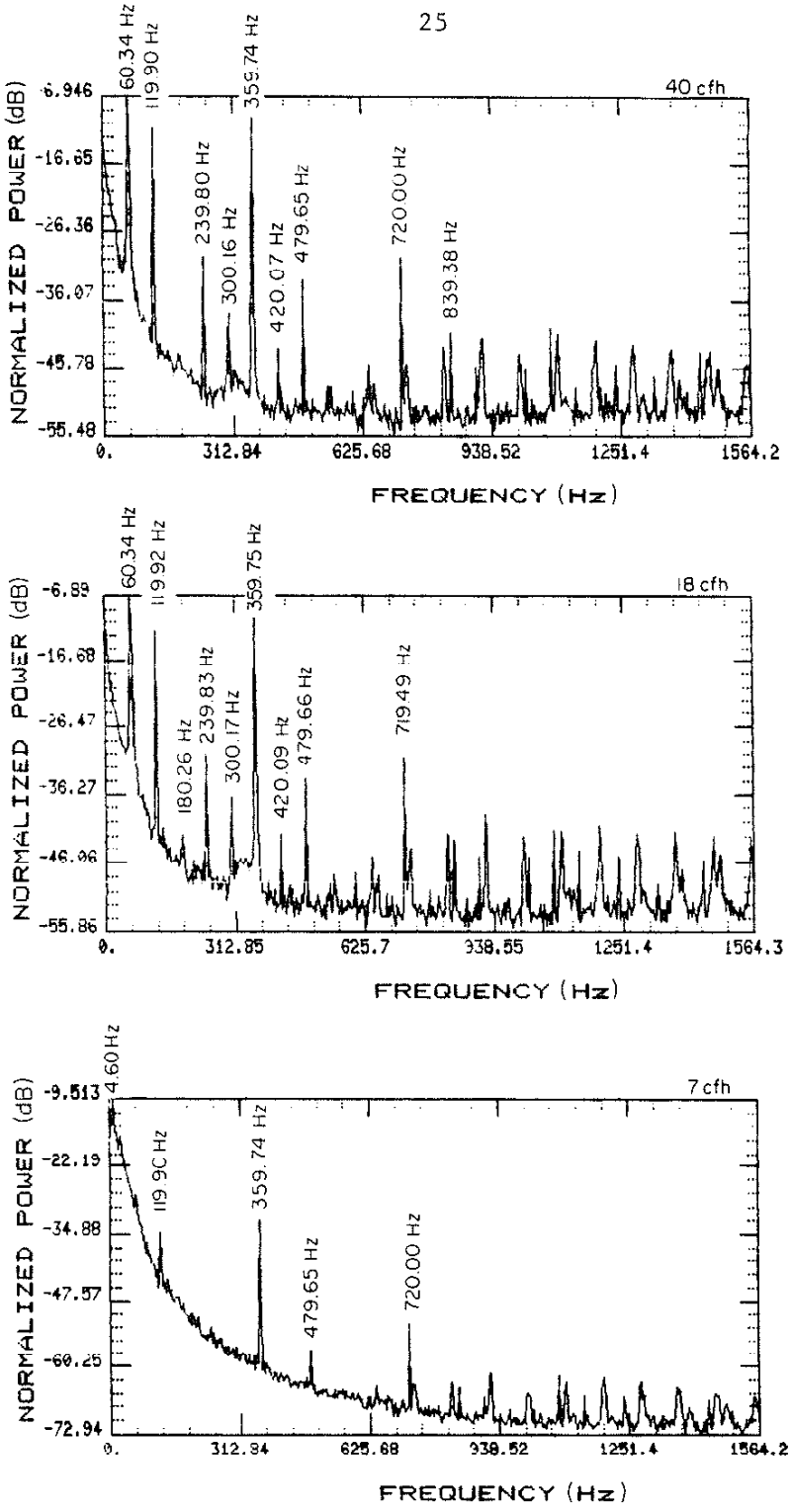

Figure 13. Power spectrum of arc current fluctuations sampled at 3.1284 kHz. (a) Optimum welding, shield gas flow rate was 40 cfh. (b) Shield gas flow rate was 18 cfh. (c) Shield gas flow rate was 7 cfh.

to the changes in the shield gas flow rate. The following formula was used to calculate this ratio

$$R_I = \frac{P_I(0.5 \text{ Hz}, 30 \text{ Hz})}{P_I(50 \text{ Hz}, 72 \text{ Hz})} \tag{7}$$

where

$$P_I(f_1,f_2) = \int_{f_1}^{f_2} df\ S_I(f)$$

$S_I(f)$ = the arc current power spectrum

I = arc current.

Figure 14 is a plot of this ratio for each data set and the three shield gas flow rates. The ratio mean for optimum welding was 0.64. When the shield gas flow rate was reduced to 18 cfh, the ratio mean rose to 0.68. The largest change in the power distribution in the power spectrum occurred when the shield gas flow rate was reduced to 7 cfh--the ratio mean increased to 37.42, a more than 4000% increase over the optimum ratio.

5.2. Arc Voltage

The fluctuations of the arc voltage were also analyzed. A typical set of voltage fluctuations versus time for three shield gas flow rates is shown in Figure 15. The arc voltage mean was 27.85 V for optimum welding. Similar to arc current, the deviation of the arc voltage from its mean was small for a stable arc. When the shield gas flow rate was reduced to 18 cfh, the voltage mean was 27.79 V. The arc voltage means for the two shield gas flow rates were similar (see Figure 16) because apparently enough Ar molecules existed in the plasma to sustain the spray transfer and the arc current density did not change appreciably (see Chapter 2). A large change in arc voltage fluctuations occurred when the flow rate was reduced to 7 cfh. The voltage mean

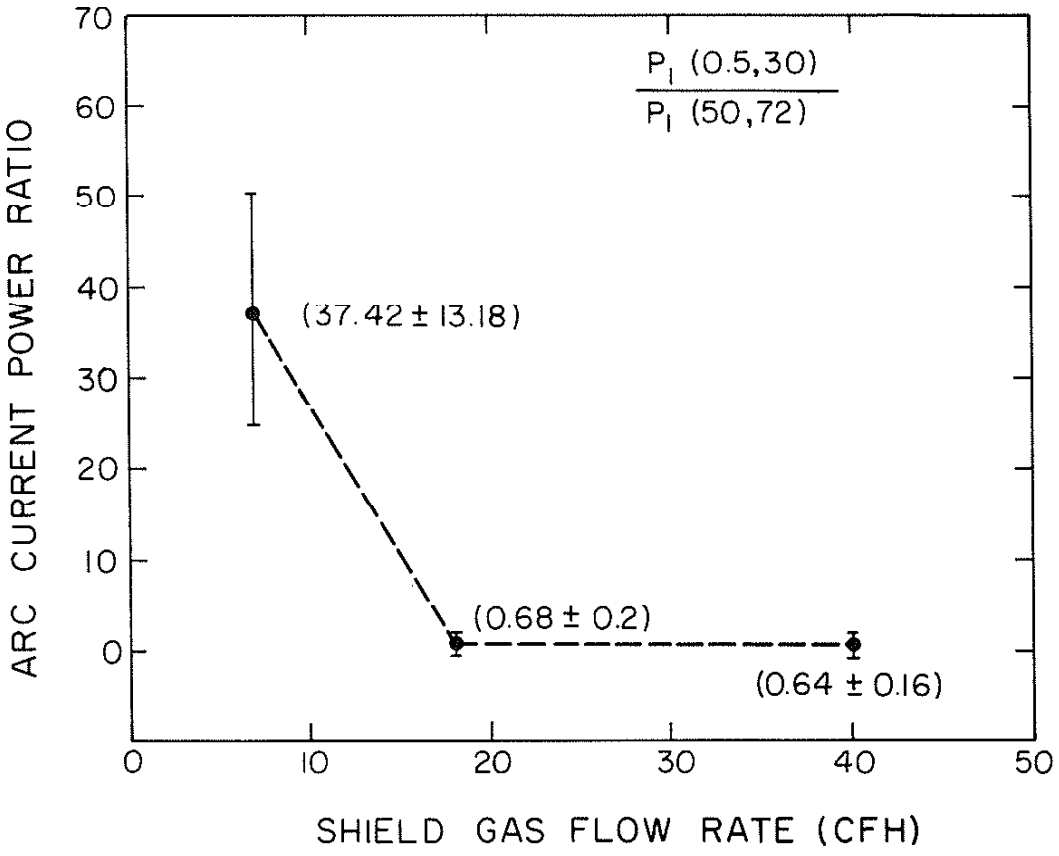

Figure 14. Arc current power ratio.

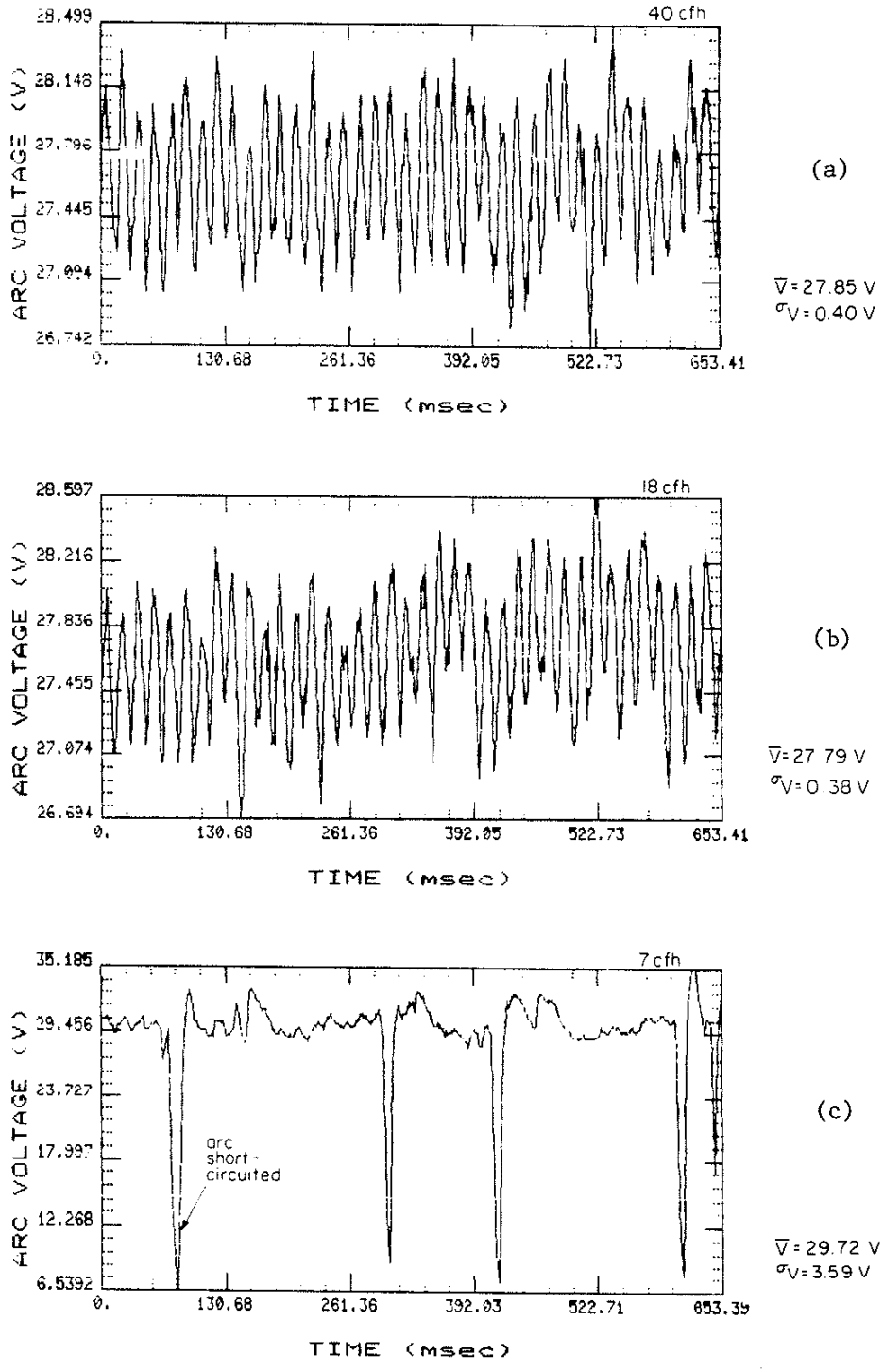

Figure 15. Arc voltage fluctuations sampled at 3.1282 kHz. (a) Optimum welding, shield gas flow rate was 40 cfh. (b) Shield gas flow rate was 18 cfh. (c) Shield gas flow rate was 7 cfh.

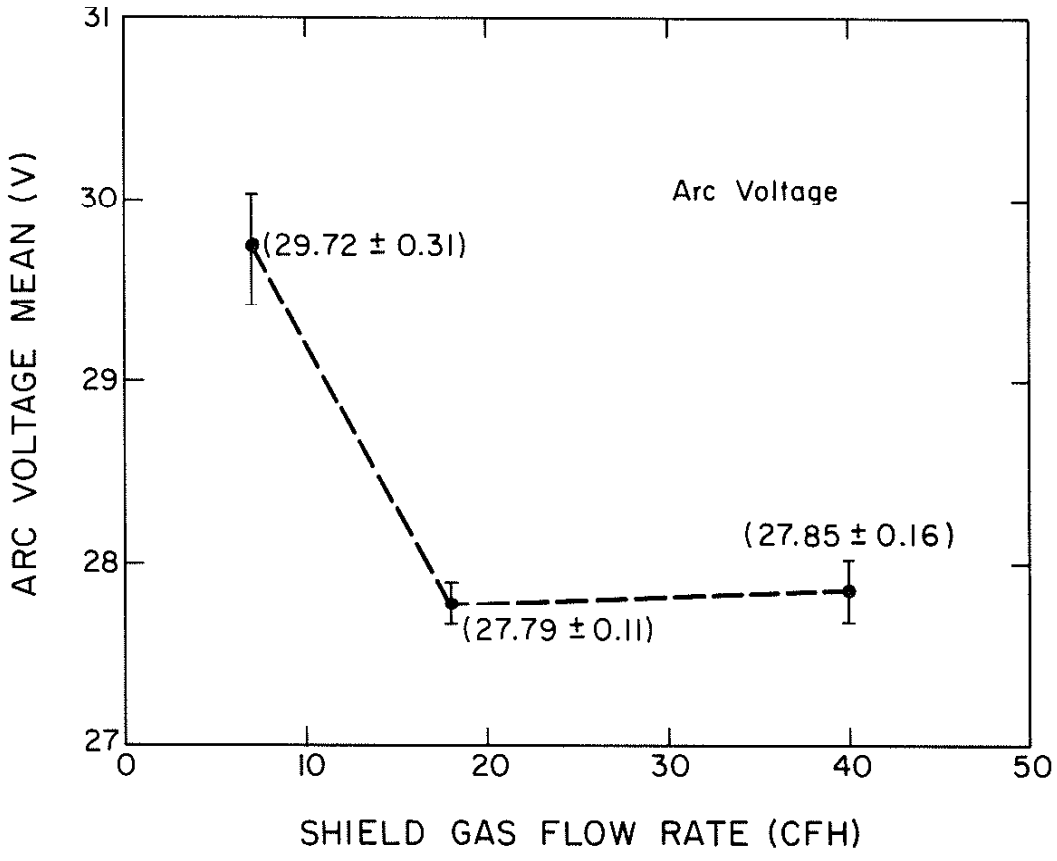

Figure 16. Arc voltage mean.

rose to 29.72 V. The sharp voltage drops (see Figure 15c) occurred because the molten metal droplets from the electrode short-circuited the arc.

A quasi-periodic signal can be seen in optimum arc voltage fluctuations (see Figure 15a). Figure 17 shows the power spectra of the arc voltage fluctuations with three different shield gas flow rates. The amplitude of the 60.33 Hz fluctuations is 11 dB higher than the amplitude of the other frequencies; this was the frequency of the dominant fluctuations observed in arc voltage fluctuations. The other distinguishable frequencies were the 60 Hz harmonics which were believed to be the result of the full-wave rectification of the three-phase AC input by the power supply, as was the case with the arc current. However, the magnitude of these 60 Hz harmonics was much smaller in arc voltage fluctuations than in arc current fluctuations. This was the result of the constant voltage power supply maintaining an approximately constant voltage by varying the current to keep a preset arc length.

The spectral slope changed significantly in the frequency range 300-360 Hz when the shield gas flow rate was reduced. Figure 18 is a plot of the frequency range 200-400 Hz for the three shield gas flow rates. Also the power below 40 Hz increased when the shield gas flow rate was reduced. This power was divided by the power in the 60 Hz signal to provide a number that would be sensitive to shield gas flow rate reduction.

$$R_V = \frac{P_V(0.5\ \text{Hz},\ 30\ \text{Hz})}{P_V(50\ \text{Hz},\ 72\ \text{Hz})} \tag{8}$$

where

$$P_V(f_1,f_2) = \int_{f_1}^{f_2} df\ S_V(f)$$

$S_V(f)$ = the arc voltage power spectrum

V = arc voltage .

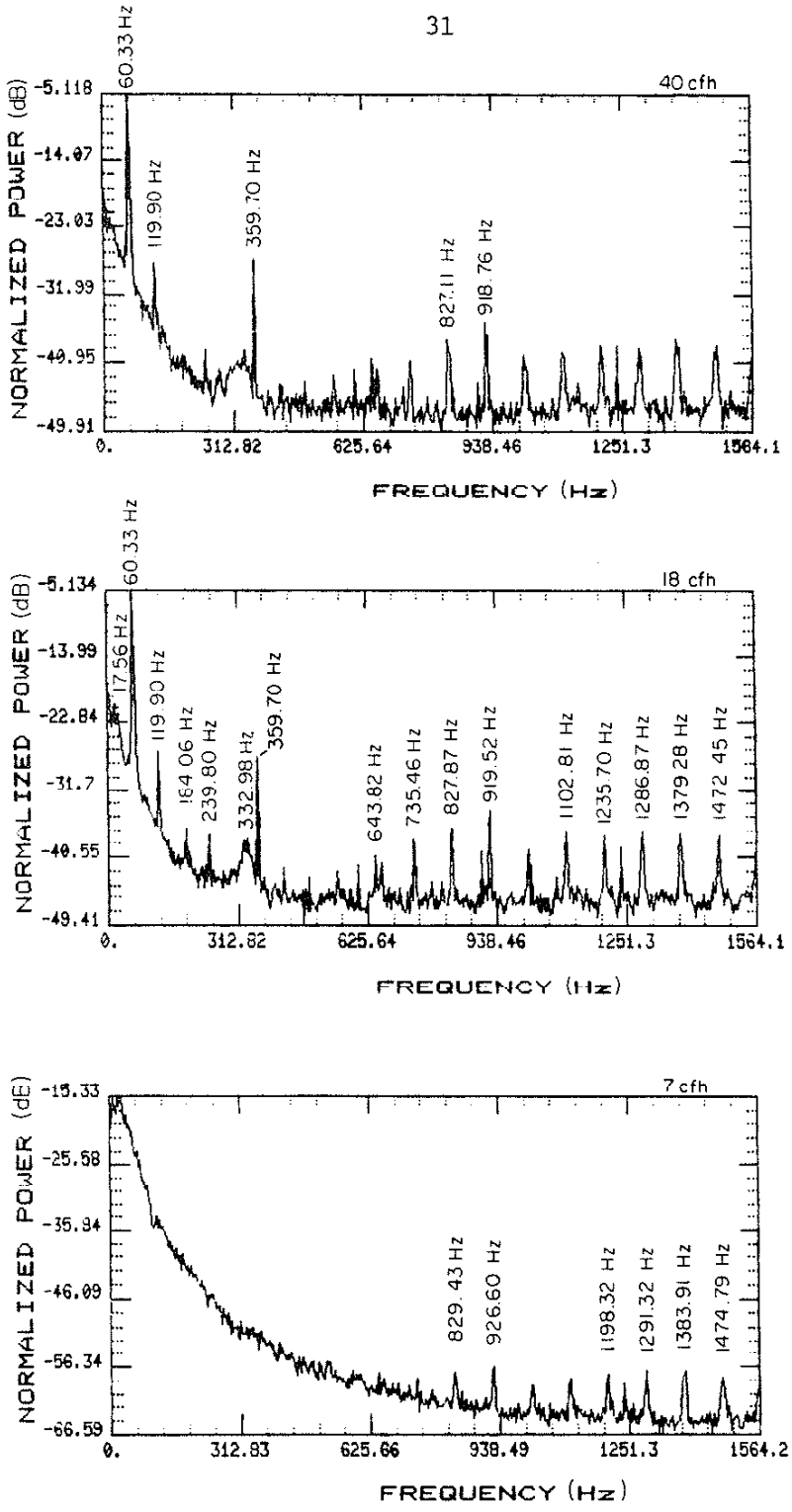

Figure 17. Power spectrum of arc voltage fluctuations sampled at 3.1282 kHz. (a) Optimum welding, shield gas flow rate was 40 cfh. (b) Shield gas flow rate was 18 cfh. (c) Shield gas flow rate was 7 cfh.

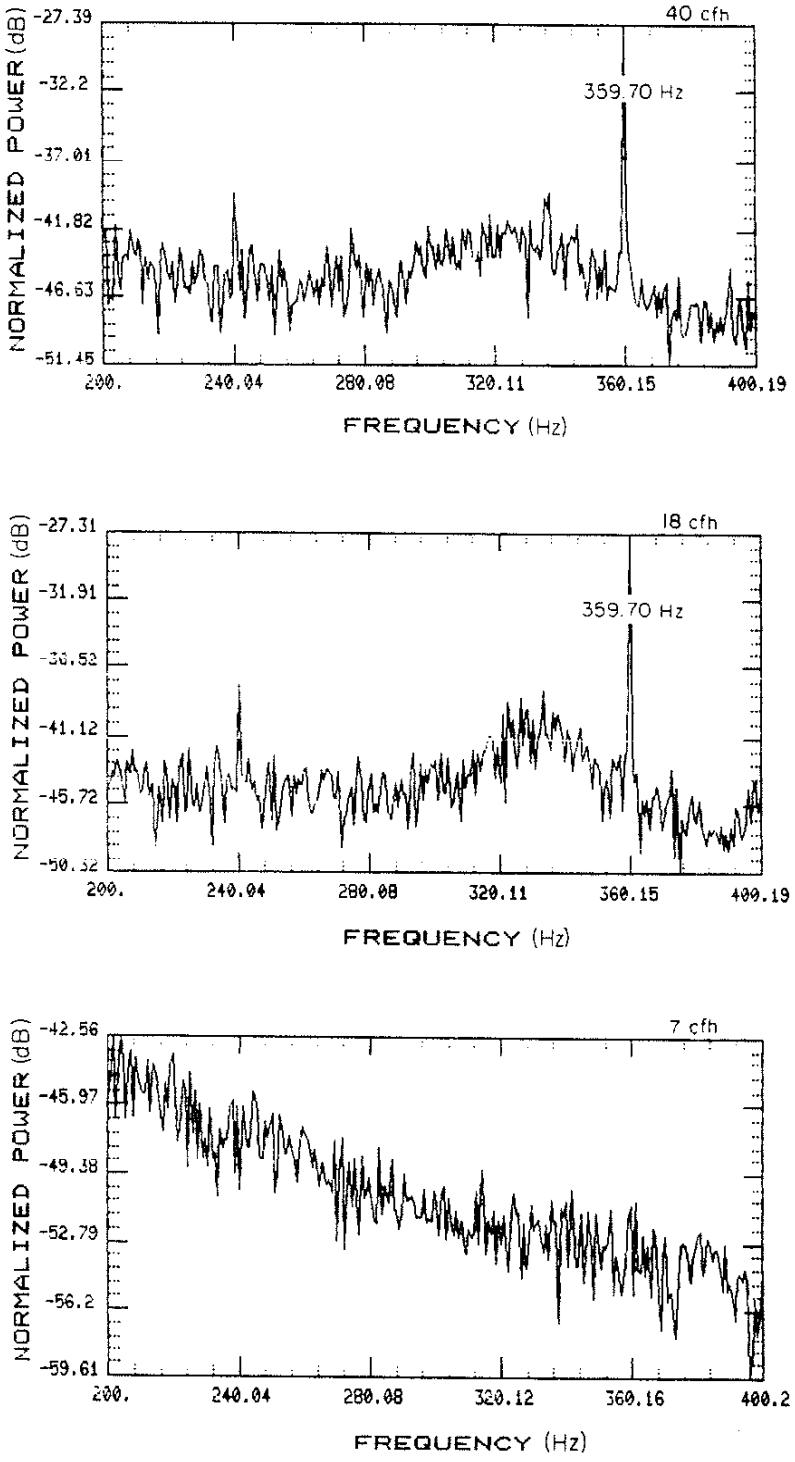

Figure 18. The 200-400 Hz region of the arc voltage fluctuations sampled at 3.1282 kHz. (a) Optimum welding, shield gas flow rate was 40 cfh. (b) Shield gas flow rate was 18 cfh. (c) Shield gas flow rate was 7 cfh.

Figure 19 is a plot of this ratio for individual data sets. The ratio mean for optimum welding was 0.21. When the shield gas flow rate was reduced to 18 cfh, the ratio mean increased to 0.25. The ratio mean increased by more than 2000% to 6.63 when the shield gas flow rate was reduced to 7 cfh.

5.3. Argon (Ar)

In addition to voltage and current, the fluctuations of the Ar emission line at 8115.311 Å (see Figure 20) [19], [20] were investigated. Since the frequency content of this signal was not known a priori, no electrical filter was used; but to avoid aliasing distortion, the signal was sampled at 20.734 kHz. The power spectra with shield gas flow rate of 40 cfh (optimum welding) and with shield gas flow rate reduced to 7 cfh are shown in Figure 21. The lower frequencies had larger magnitudes. The shield gas flow rate reduction caused an increase in low frequency--below 100 Hz--power and a decrease in the power of frequencies above 100 Hz, especially in the 300-360 Hz region which was reduced by about 10 dB.

To study the variations with higher resolution, the sampling frequency was lowered. Figure 22 shows the Ar line fluctuations with three shield gas flow rates. These fluctuations appeared random; hence, the mean and standard deviations of each data set were calculated (see Figure 23). The Ar line fluctuation mean for optimum welding was 1.47 V and the normalized standard deviation of the mean was 0.044. Although the fluctuations appeared random, the mean of the process was almost constant. The mean when the shield gas flow rate was reduced to 18 cfh was 1.40 V. This was slightly lower than the fluctuation intensity mean for the optimum shield gas flow rate of 40 cfh. When the shield gas flow rate was reduced to 7 cfh, the intensity mean dropped to 0.10 V. This was less than one tenth of the Ar line intensity mean for optimum welding.

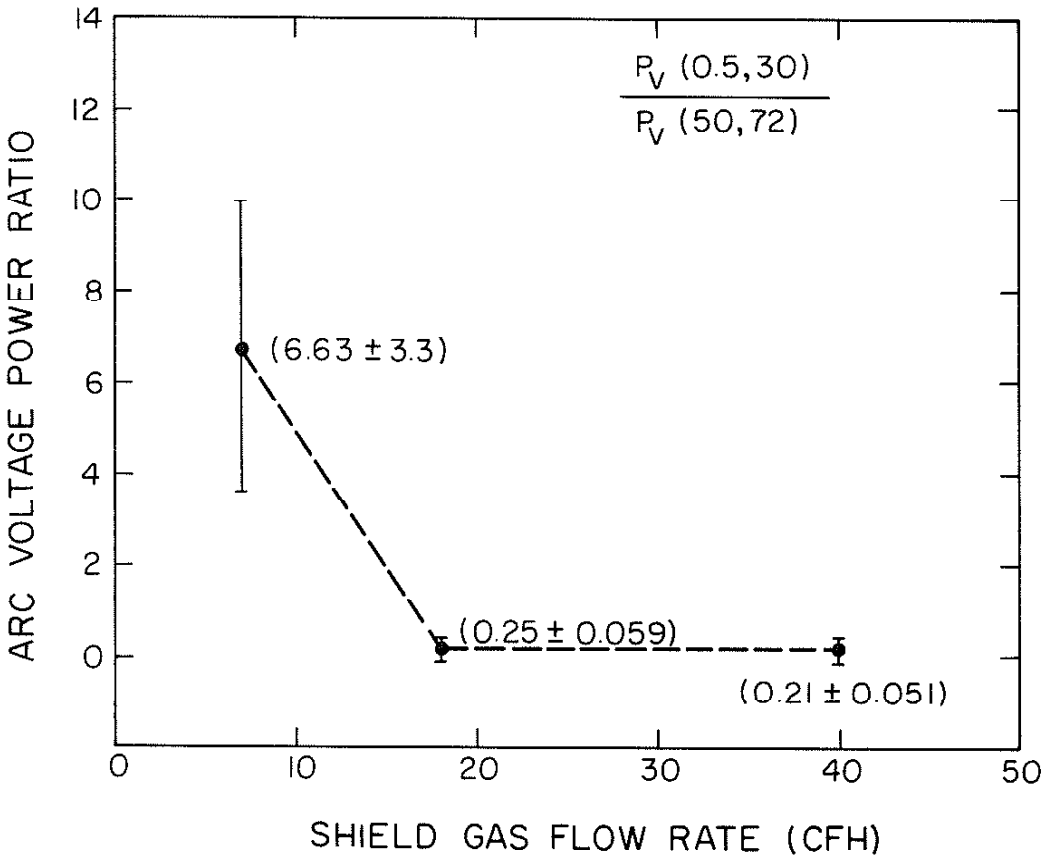

Figure 19. Arc voltage power ratio.

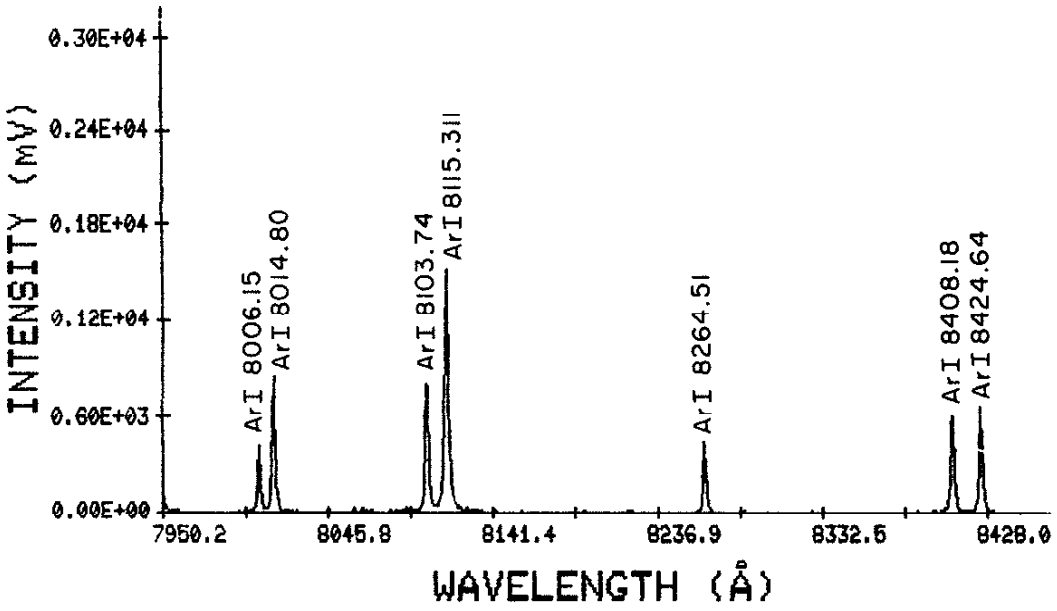

Figure 20. Optical emission spectrum of the weld arc in the vicinity of 8115.311 Å.

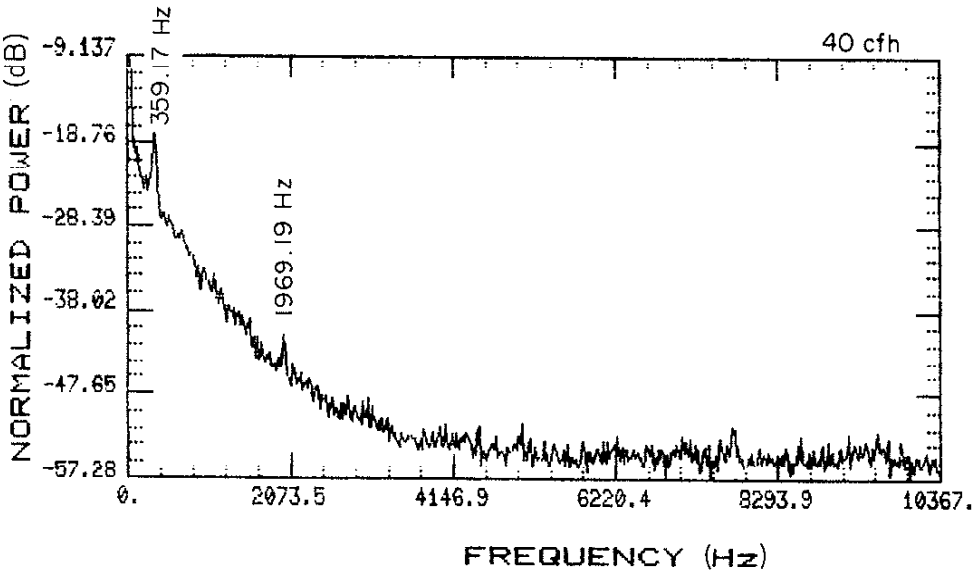

(a)

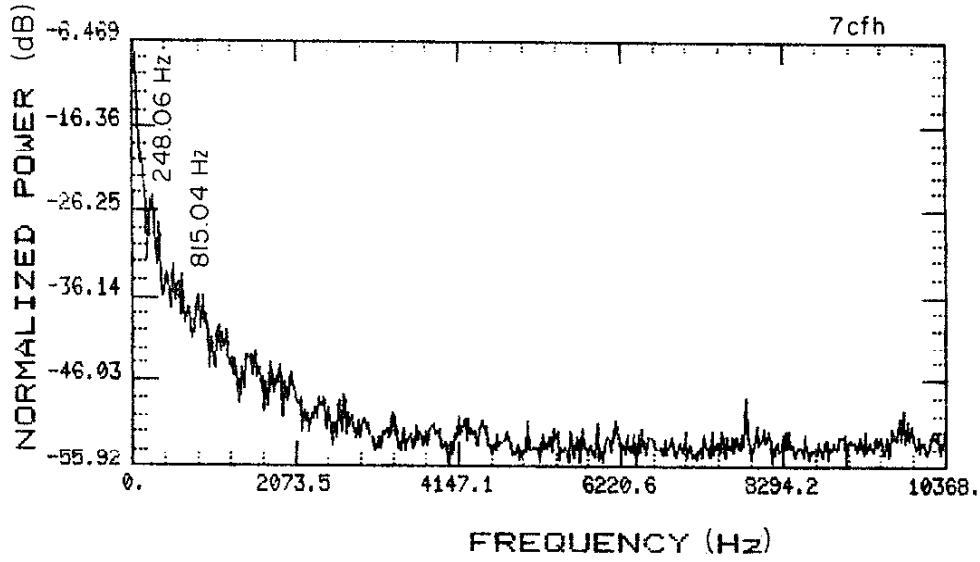

(b)

Figure 21. Power spectrum of Ar line intensity fluctuations at 8115.311 Å, sampled at 20.734 kHz. (a) Optimum welding, shield gas flow rate was 40 cfh. (b) Shield gas flow rate was 7 cfh.

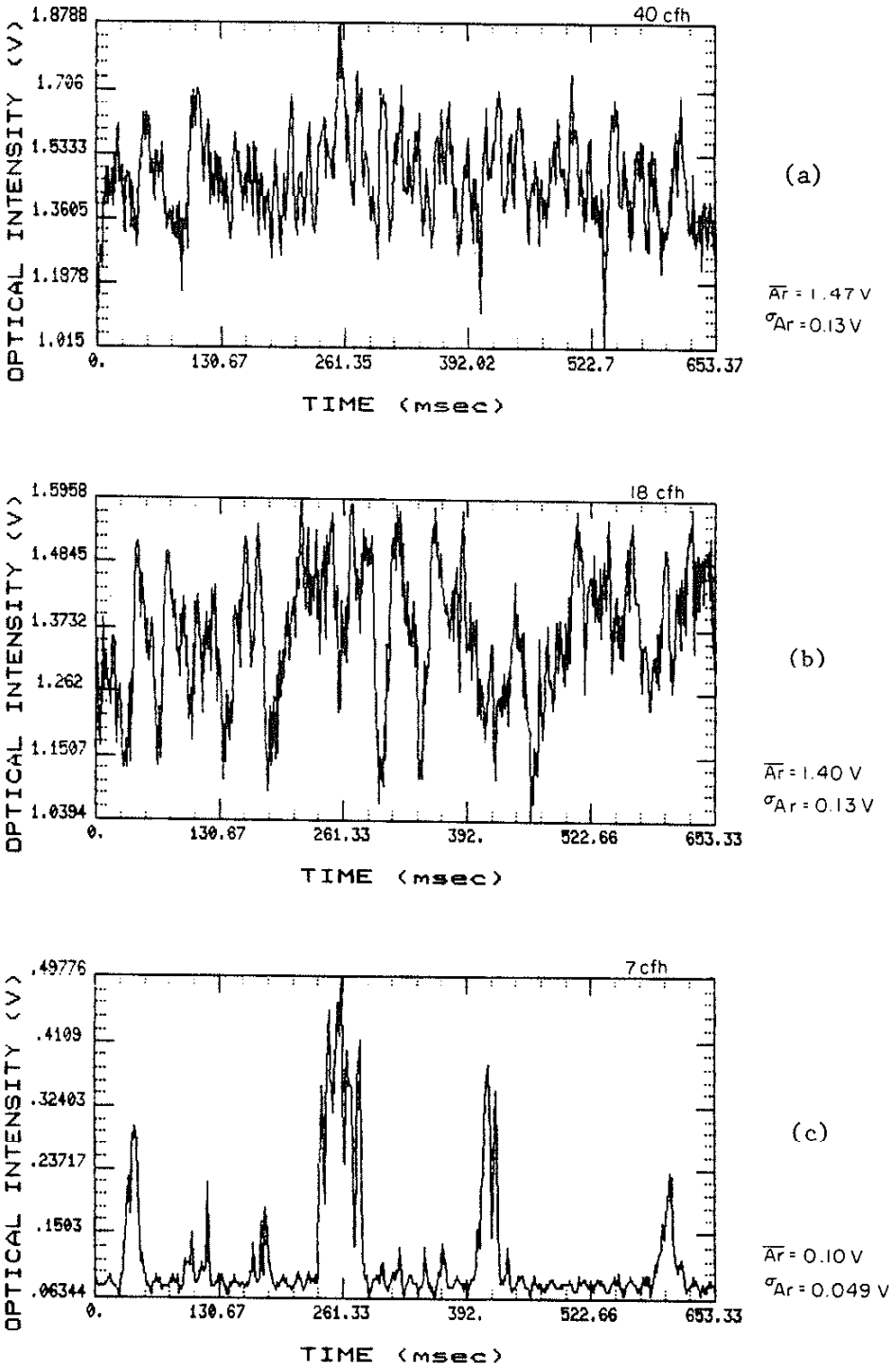

Figure 22. Ar line intensity fluctuations at 8115.311 Å, sampled at 3.1284 kHz. (a) Optimum welding, shield gas flow rate was 40 cfh. (b) Shield gas flow rate was 18 cfh. (c) Shield gas flow rate was 7 cfh.

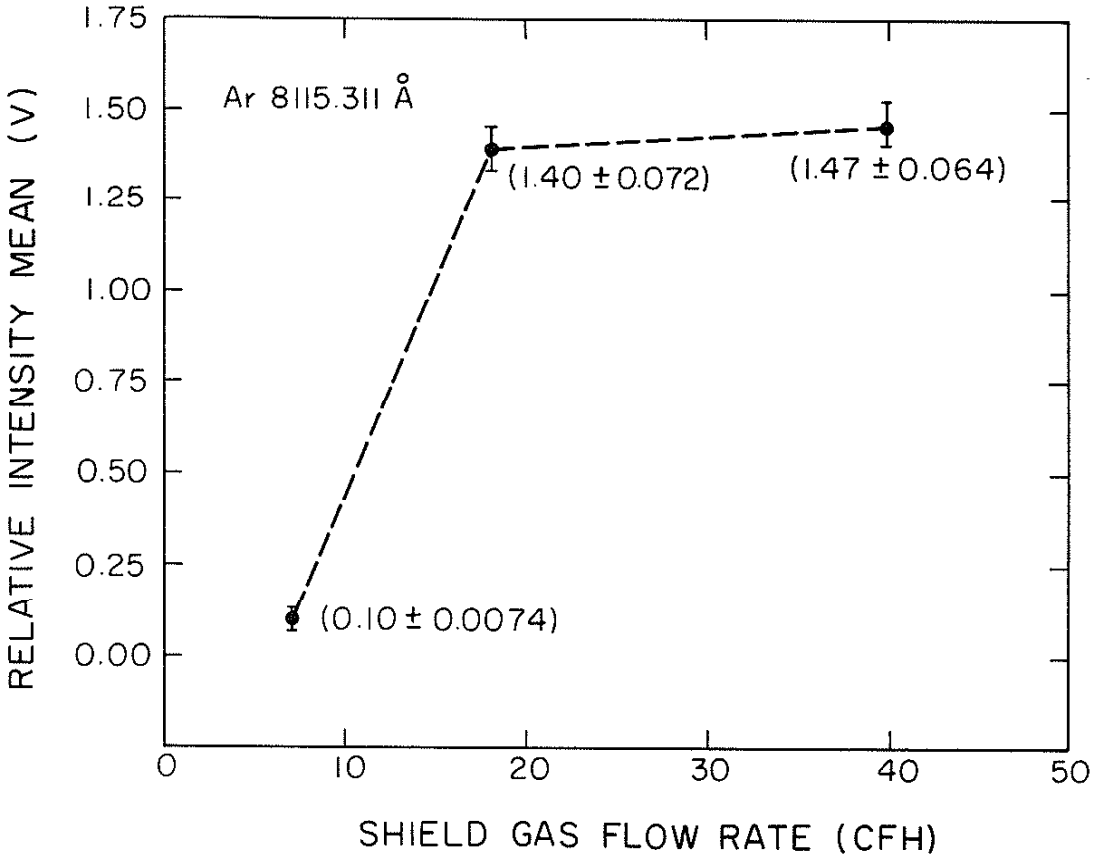

Figure 23. Ar line intensity mean at 8115.311 Å.

The power spectra of Ar line fluctuations are shown in Figure 24. The magnitudes of the 60 Hz fluctuations and its harmonics are much weaker in the Ar power spectra when compared to the arc current and voltage power spectra. Theoretical studies have shown [21] that the amplitude of the weld bead temperature oscillations decreased as the frequency of welding current pulses was increased beyond a certain value which depended on the welding type and the material used. The 60 Hz fluctuations of the arc current seemed to be beyond the plasma temperature sensitivity range to the arc current fluctuations.

No single frequency was dominant in the power spectra. The Ar power spectrum was monotonically decreasing, except for the 300-360 Hz region. This region exhibited the largest change in slope of power spectra when the shield gas flow rate was reduced (see Figure 25). This was similar to the behavior of the corresponding frequency ranges in current and voltage variations. The power in this broad-band signal dropped as the shield gas flow rate was reduced; therefore, the ratio of the low frequency power to the power in this broadband signal could provide a numerical value sensitive to the shield gas flow rate reduction.

$$R_{Ar} = \frac{P_{Ar}(0.5 \text{ Hz}, 30 \text{ Hz})}{P_{Ar}(250 \text{ Hz}, 400 \text{ Hz})} \tag{9}$$

where

$$P_{Ar}(f_1, f_2) = \int_{f_1}^{f_2} df \; S_{Ar}(f)$$

$S_{Ar}(f)$ = power spectrum of Ar fluctuations.

The value of R_{Ar} for each data set is plotted in Figure 26. The ratio mean for shield gas flow rate of 40 cfh was 10.87. When the shield gas flow rate was reduced to 18 cfh, the ratio mean rose to 11.93. The ratio mean increased to 88.91 when the shield gas flow rate was reduced to 7 cfh. The power ratio mean

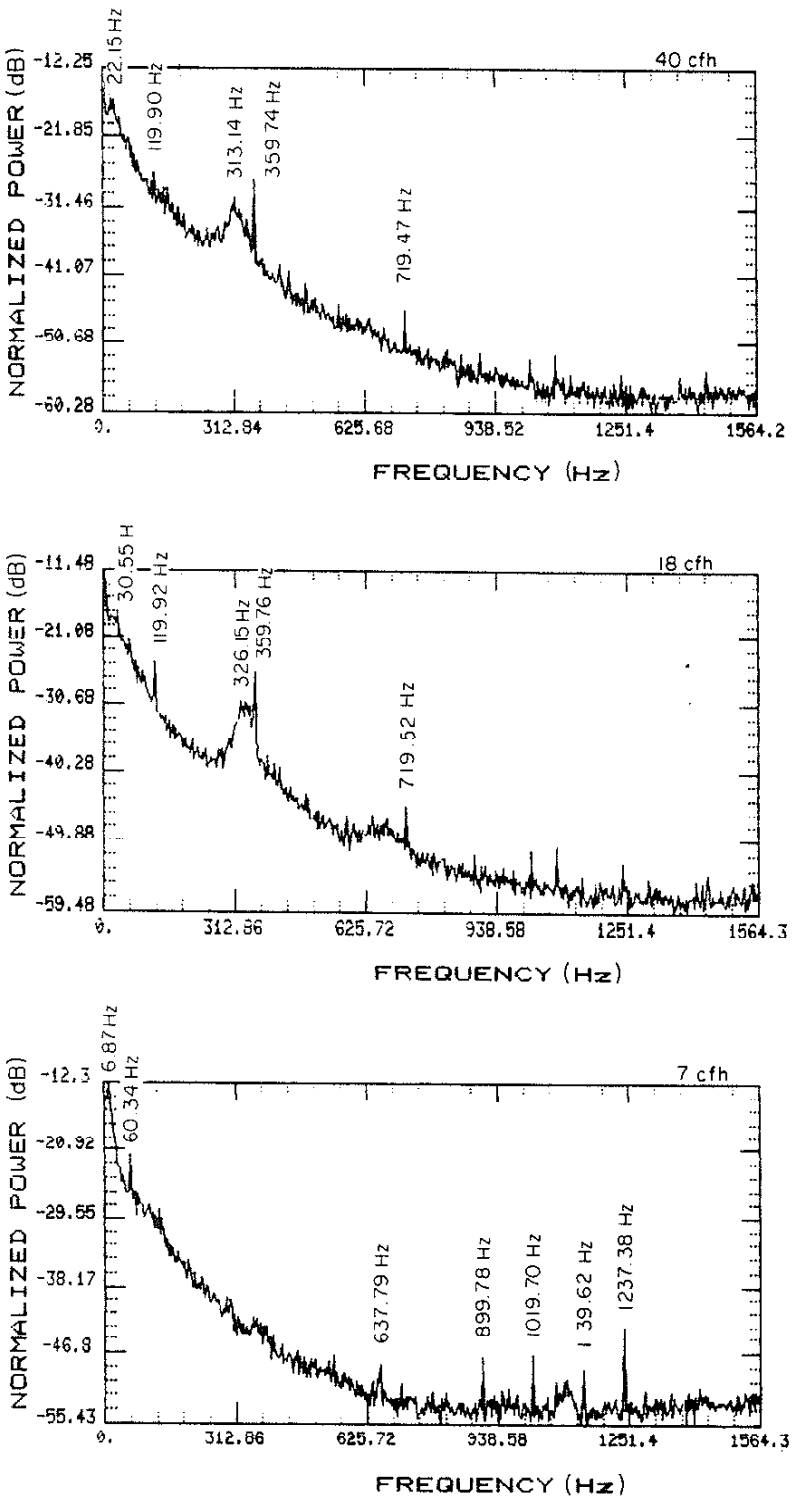

Figure 24. Power spectrum of Ar line intensity fluctuations at 8115.311 Å, sampled at 3.1284 kHz. (a) Optimum welding, shield gas flow rate was 40 cfh. (b) Shield gas flow rate was 18 cfh. (c) Shield gas flow rate was 7 cfh.

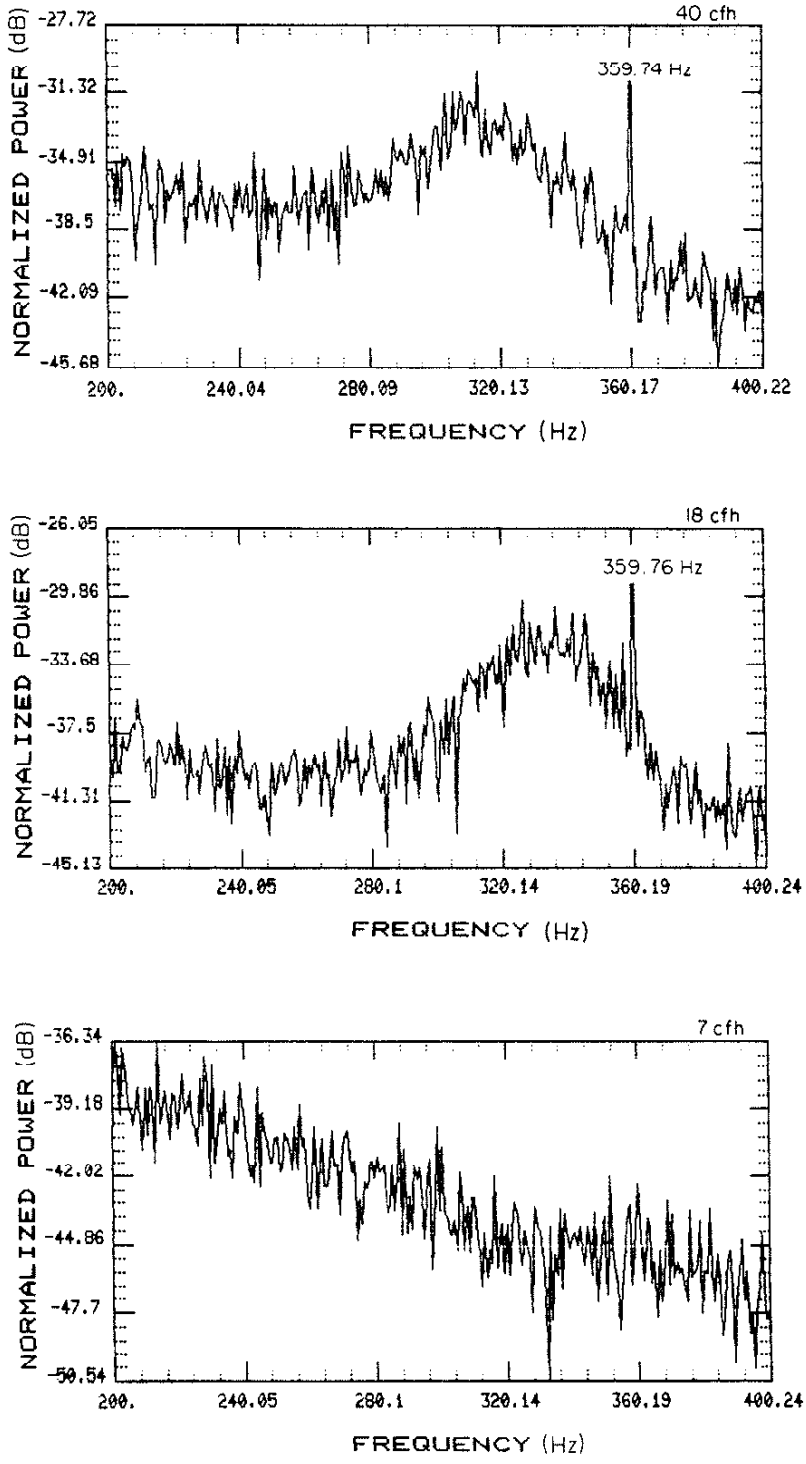

Figure 25. The 200 - 400 Hz region of the Ar line fluctuations sampled at 3.1284 kHz. (a) Optimum welding, shield gas flow rate was 40 cfh. (b) Shield gas flow rate was 18 cfh. (c) Shield gas flow rate was 7 cfh.

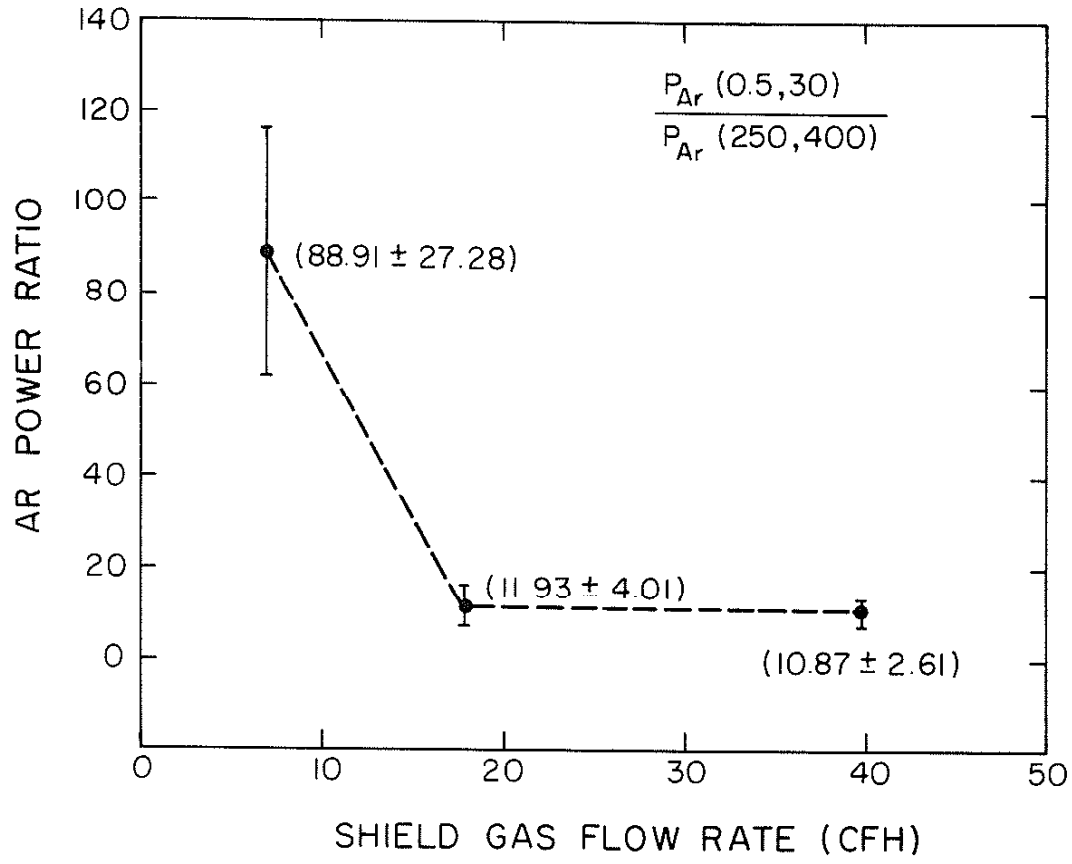

Figure 26. Ar power ratio.

increased when the shield gas flow rate was reduced, with the largest increase occurring when the shield gas flow rate was reduced beyond 18 cfh.

5.4. Iron (Fe)

The fluctuations of the Fe line at 4383.544 Å [19], [20] were also analyzed. Figure 27 is a plot of the optical emission spectrum of the weld arc in the vicinity of this line. Initially, the signal was sampled at 20.678 kHz to preserve its entire frequency content. The power spectra for the shield gas flow rate of 40 cfh and 7 cfh are shown in Figure 28. The slope of the power spectra increased when the shield gas flow rate was reduced. It was also observed that low frequency power below approximately 250 Hz increased and the spectral power beyond approximately 250 Hz decreased.

To increase the power spectral resolution, the sampling frequency was lowered to 3.1288 kHz. The fluctuations of Fe emissions at 4383.544 Å sampled at this frequency are shown in Figure 29. These fluctuations appeared random, so the mean and standard deviation of the data sets were calculated. The Fe line intensity means of individual data sets for the three shield gas flow rates are shown in Figure 30. The intensity mean was 0.63 V for optimum shield gas flow rate of 40 cfh. The mean dropped to 0.57 V for the reduced shield gas flow rate of 18 cfh. The largest change occurred when the shield flow rate was further reduced to 7 cfh. The Fe line intensity mean dropped to 0.16 V.

The power spectra of Fe fluctuations are shown in Figure 31. Although the fluctuations appeared random, they had well-defined power spectra. The 60 Hz and its harmonics were either missing or had much smaller amplitudes than was the case for the arc voltage and the arc current fluctuations. This was caused by low plasma temperature sensitivity to very rapid changes in arc current. This same phenomenon was observed in Ar line fluctuations (see

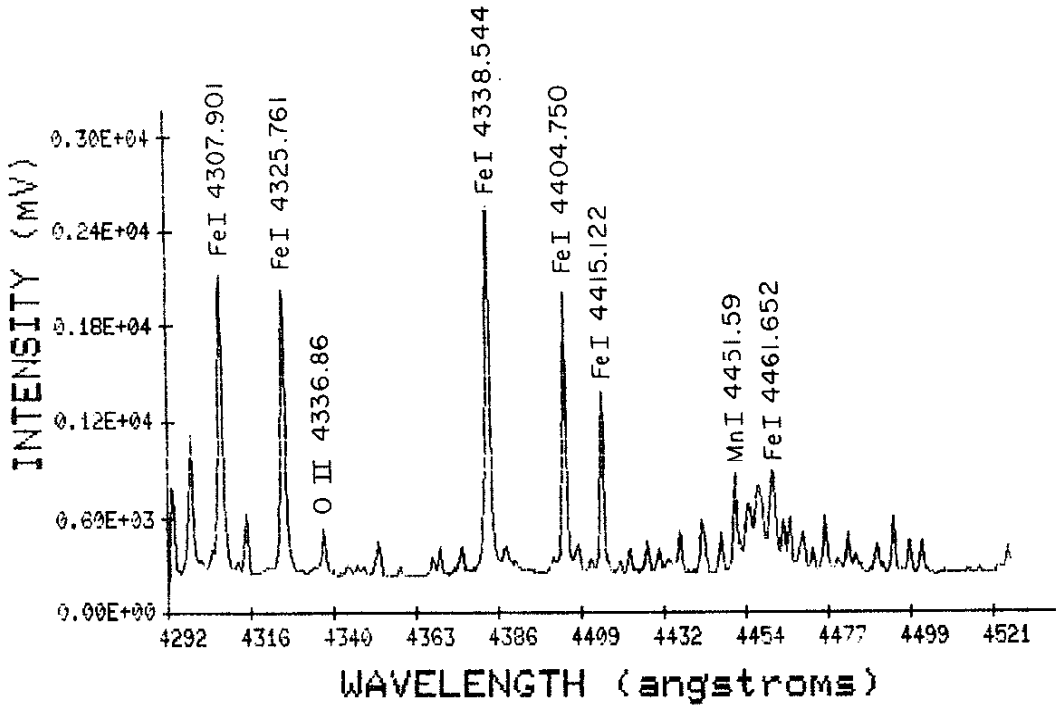

Figure 27. Optical emission spectrum of the weld arc in the vicinity of 4383.544 Å.

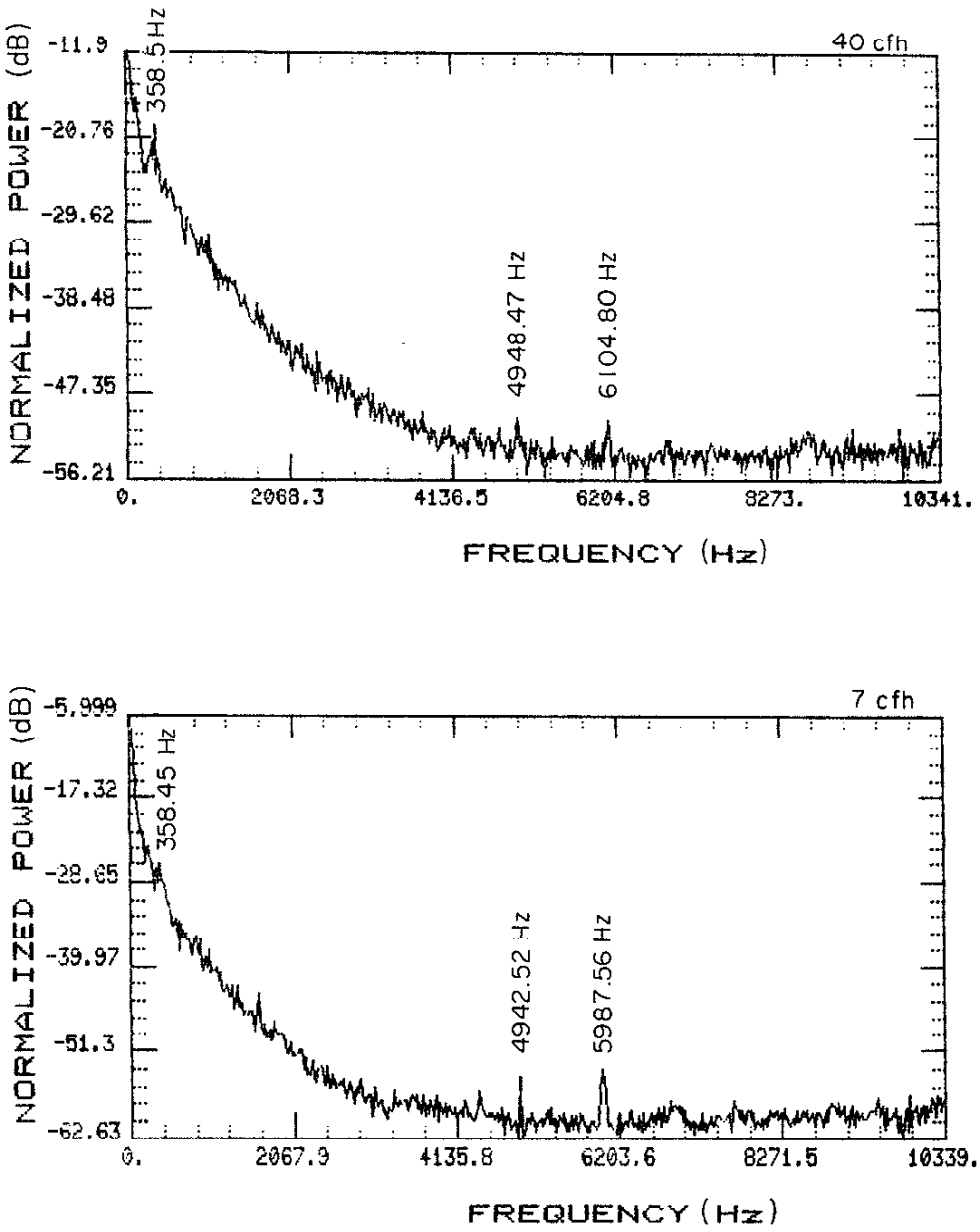

Figure 28. Power spectrum of Fe line intensity fluctuations at 4383.544 Å, sampled at 20.678 kHz. (a) Optimum welding, shield gas flow rate was 40 cfh. (b) Shield gas flow rate was 7 cfh.

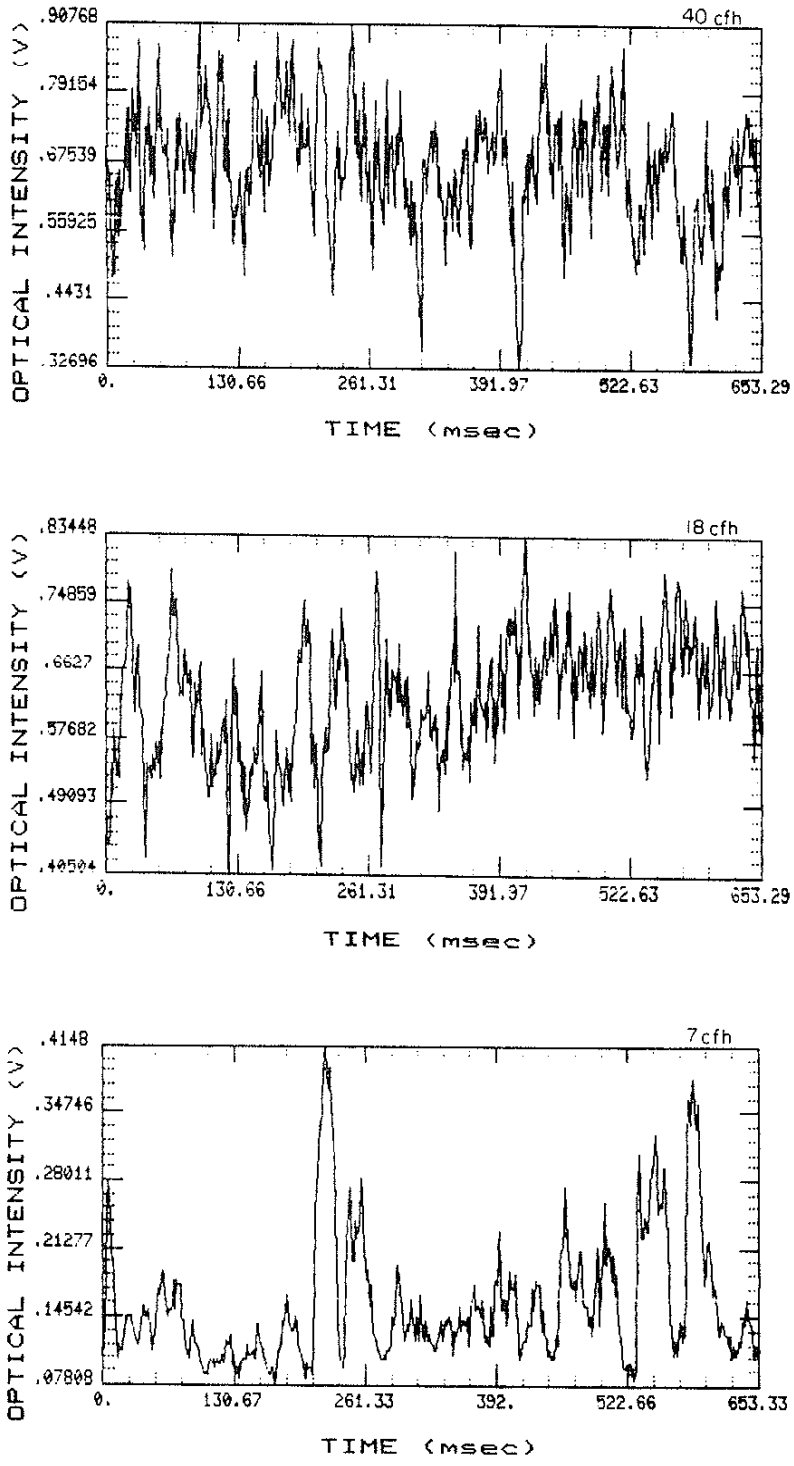

Figure 29. Fe line intensity fluctuations at 4383.544 Å, sampled at 3.1288 kHz. (a) Optimum welding, shield gas flow rate was 40 cfh. (b) Shield gas flow rate was 18 cfh. (c) Shield gas flow rate was 7 cfh.

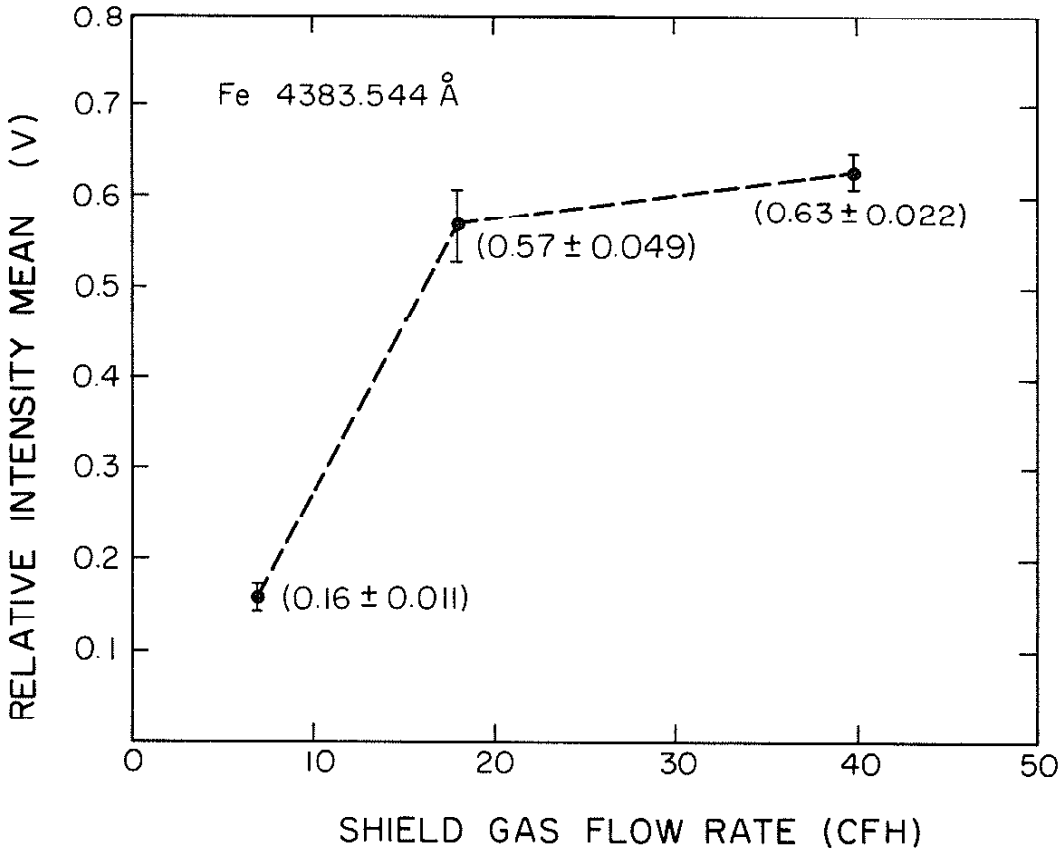

Figure 30. Fe line intensity mean at 4383.544 Å.

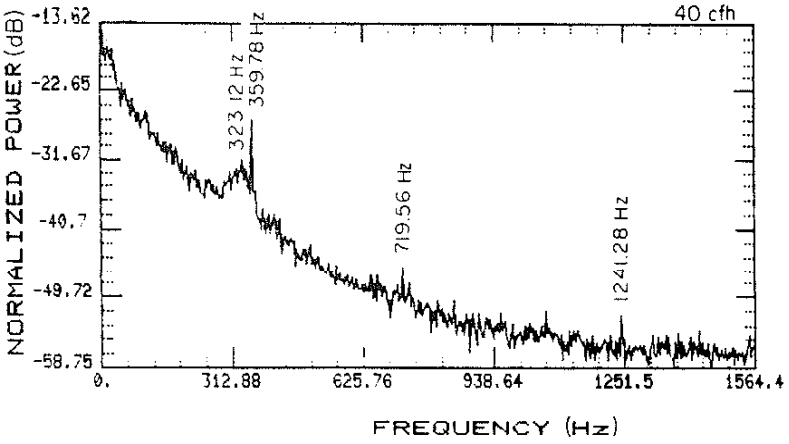

(a)

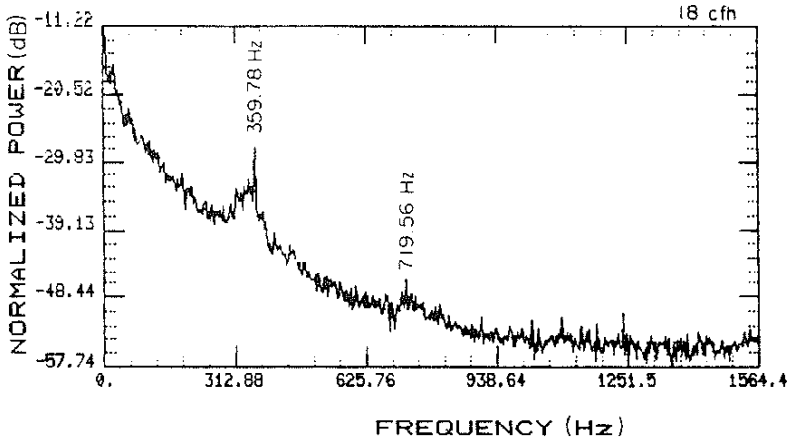

(b)

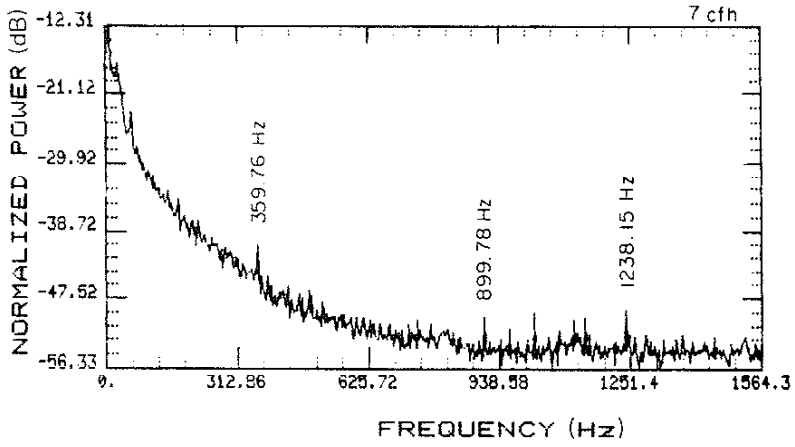

(c)

Figure 31. Power spectrum of Fe line intensity fluctuations at 4383.544 Å, sampled at 3.1288 kHz. (a) Optimum welding, shield gas flow rate was 40 cfh. (b) Shield gas flow rate was 18 cfh. (c) Shield gas flow rate was 7 cfh.

Figure 24). As seen in Figure 32, the slope of the 300-360 Hz region changed drastically when the shield gas flow rate was reduced. The power in this frequency range reduced as the shield gas flow rate was reduced. This power could be used in the power ratio to get a numerical value representing the shield gas flow rate. The power ratio was chosen as

$$R_{Fe} = \frac{P_{Fe}(0.5 \text{ Hz}, 30 \text{ Hz})}{P_{Fe}(250 \text{ Hz}, 400 \text{ Hz})} \tag{10}$$

where

$$P_{Fe}(f_1,f_2) = \int_{f_1}^{f_2} df\ S_{Fe}(f)$$

$S_{Fe}(f)$ = the Fe line fluctuations' power spectrum.

The ratio for each set for the three experimental conditions is plotted in Figure 33. The ratio mean for optimum welding was 12.73. The ratio mean increased to 17.14 when the shield gas flow rate was reduced to 18 cfh. The ratio mean increased to 116.18--a more than 500% increase from the optimum ratio--when the shield gas flow rate was reduced to 7 cfh. The ratio mean increased as the shield gas flow rate was decreased, and became more sensitive to the shield gas flow rate reduction after it was reduced beyond 18 cfh.

The smoke produced by the welding process should be taken into account when interpreting these power ratios. The optical radiation from the arc plasma was scattered by the smoke particles; therefore, changes in the density and thickness of the smoke were responsible for some of the intensity fluctuations in the measured optical intensity [3]. However, the trend in the power ratios was similar in all of the parameters monitored, including the voltage and the current. Therefore, it is expected that the trend in the power ratios calculated from the detected optical emissions is indicative of the plasma radiation behavior.

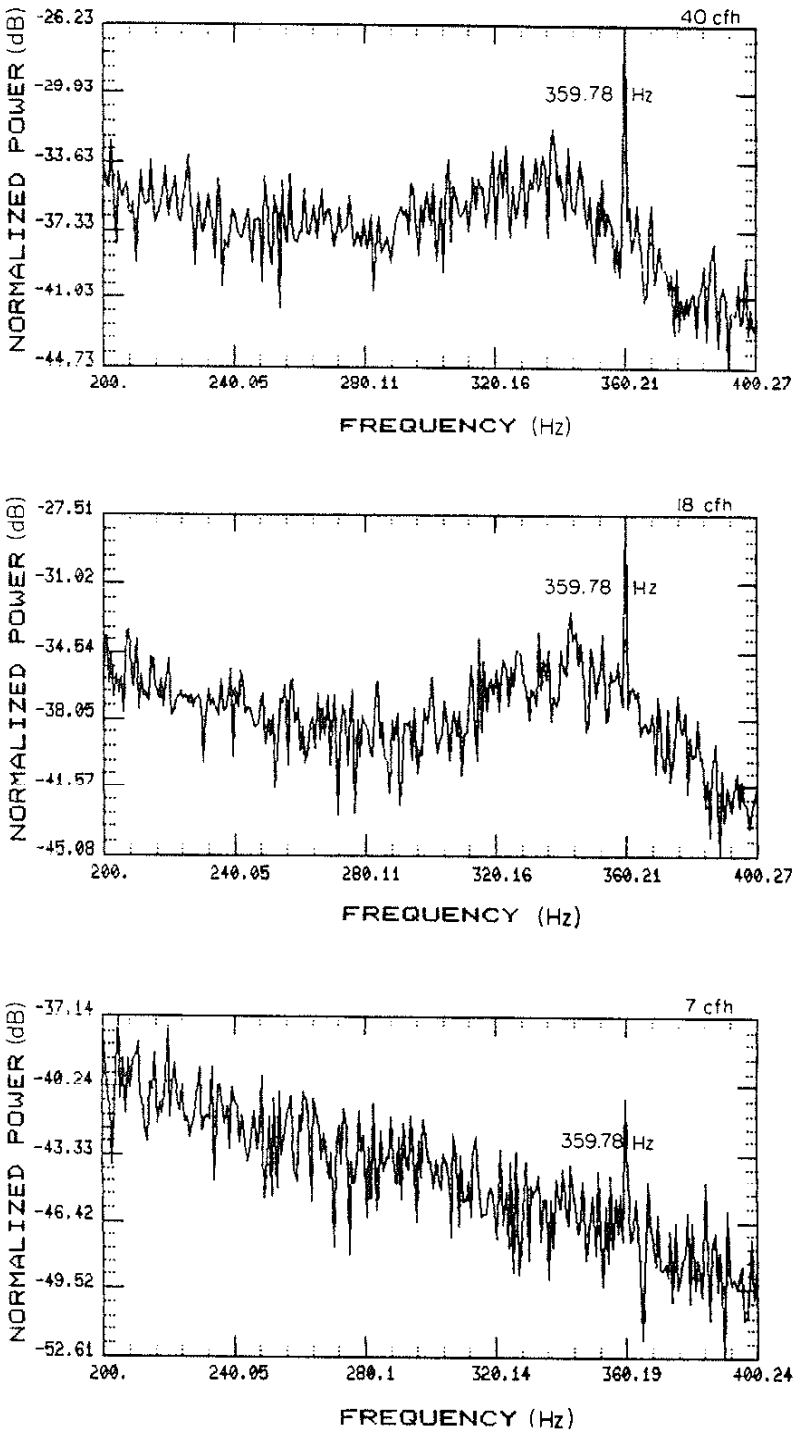

Figure 32. The 200 - 400 Hz region of the Fe line fluctuations sampled at 3.1288 kHz. (a) Optimum welding, shield gas flow rate was 40 cfh. (b) Shield gas flow rate was 18 cfh. (c) Shield gas flow rate was 7 cfh.

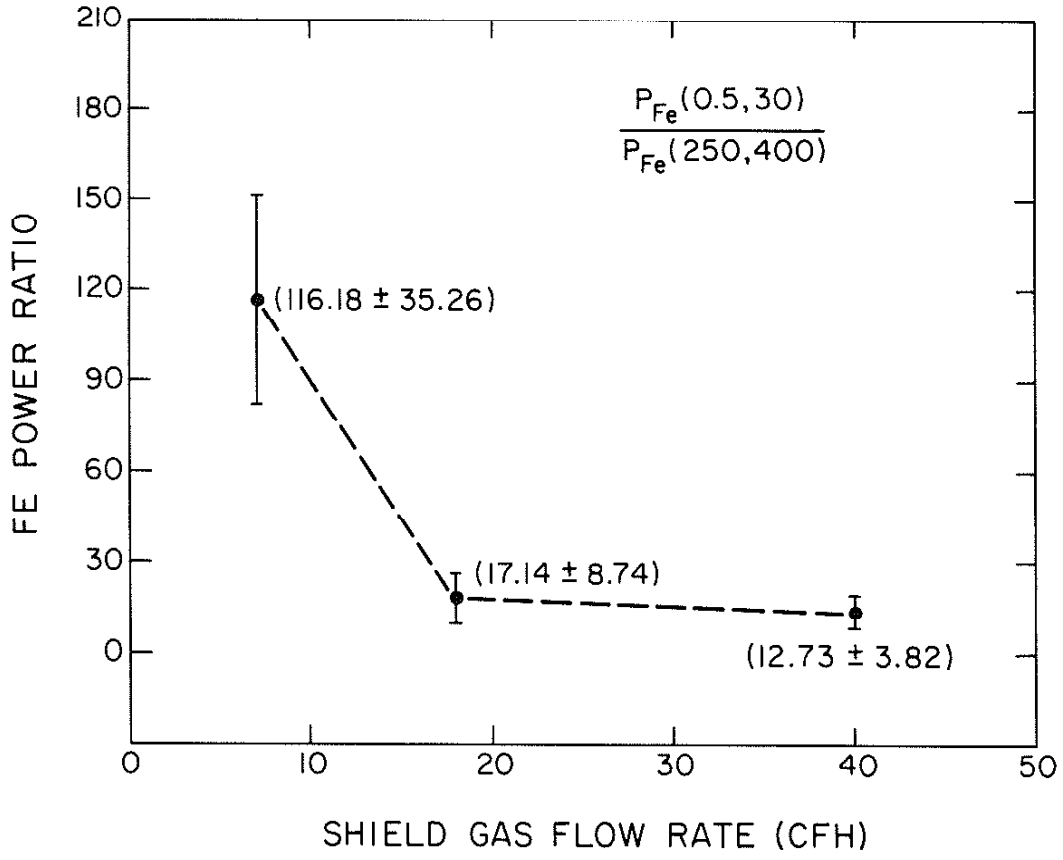

Figure 33. Fe power ratio.

Table 2 lists the statistical parameters of the weld arc current, voltage, and optical emissions. The statistical parameters of the power ratios are summarized in Table 3.

TABLE 2

STATISTICAL PARAMETERS OF WELD ARC CURRENT, VOLTAGE, AND OPTICAL EMISSIONS

EXPERIMENTAL VARIABLE	SHIELD GAS FLOW RATE	MEAN	STANDARD DEVIATION	NORMALIZED STANDARD DEVIATION
		$\overline{I}$ (A)	σ_I (A)	$\sigma_I/\overline{I}$
I	40 cfh	328.40	2.66	0.0081
	18	321.73	3.11	0.0097
	7	272.17	42.55	0.1563
		$\overline{V}$ (V)	σ_V (V)	$\sigma_V/\overline{V}$
V	40	27.85	0.40	0.014
	18	27.79	0.38	0.014
	7	29.72	3.59	0.121
		$\overline{Ar}$ (V)	σ_{Ar} (V)	$\sigma_{Ar}/\overline{Ar}$
Ar 8115.311 Å	40	1.47	0.13	0.088
	18	1.40	0.13	0.093
	7	0.10	0.049	0.49
		$\overline{Fe}$ (r)	σ_{Fe} (V)	$\sigma_{Fe}/\overline{Fe}$
Fe 4383.544 Å	40	0.63	0.10	0.16
	18	0.57	0.088	0.15
	7	0.16	0.058	0.36

TABLE 3

STATISTICAL PARAMETERS OF POWER RATIOS FROM WELD ARC CURRENT, VOLTAGE, AND OPTICAL EMISSIONS

EXPERIMENTAL VARIABLE	SHIELD GAS FLOW RATE	POWER RATIO MEAN	STANDARD DEVIATION	NORMALIZED STANDARD DEVIATION	DEFINITION
		$\overline{R}_I$	σ_{R_I}	$\sigma_{R_I}/\overline{R}_I$	
I	40 cfh	0.64	0.16	0.25	$R_I = \frac{P_I(0.5,30)}{P_I(50,72)}$
	18	0.68	0.20	0.29	
	7	37.42	13.18	0.35	
		$\overline{R}_V$	σ_{R_V}	$\sigma_{R_V}/\overline{R}_V$	
V	40	0.21	0.051	0.24	$R_V = \frac{P_V(0.5,30)}{P_V(50,72)}$
	18	0.25	0.059	0.24	
	7	6.63	3.30	0.50	
		$\overline{R_{Ar}}$	$\sigma_{R_{Ar}}$	$\sigma_{R_{Ar}}/\overline{R_{Ar}}$	
Ar 8115.311 Å	40	10.87	2.61	0.24	$R_{Ar} = \frac{P_{Ar}(0.5,30)}{P_{Ar}(250,400)}$
	18	11.93	4.01	0.34	
	7	88.91	27.28	0.31	
		$\overline{R_{Fe}}$	$\sigma_{R_{Fe}}$	$\sigma_{R_{Fe}}/\overline{R_{Fe}}$	
Fe 4383.544 Å	40	12.73	3.82	0.30	$R_{Fe} = \frac{P_{Fe}(0.5,30)}{P_{Fe}(250,400)}$
	18	17.14	8.74	0.51	
	7	116.18	35.26	0.30	

6. CONCLUSION

The time fluctuations of Ar and Fe lines appeared random but the relative magnitudes of the frequency components in the fluctuations were approximately the same in repeated experiments. The power distribution in the power spectrum was indicative of the shield gas flow rate. A ratio of the power in two frequency bands, whose magnitude had opposite response to the shield gas flow rate reduction, represented the shield gas flow rate.

The fluctuations of current and voltage were dominated by 60 Hz and its harmonics, resulting from the rectification of the line voltage by the welder power supply. These dominant fluctuations in arc current and in arc voltage were not present in optical intensity fluctuations. Theoretical studies had shown that the plasma temperature has low sensitivity to high frequency fluctuations in current.

Although the experiments were conducted by reducing the shield gas flow rate, incomplete shield gas coverage due to slight breezes or other factors should be detectable. If Ar is not present in the shield gas, the metal transfer would be different, leading to different fluctuation patterns, e.g., CO_2 shield gas results in globular metal transfer [4]. If the electrode is not the filler metal, as in gas tungsten arc welding, a similar analytical method would be applicable because the current stability is partially dependent on the uniform conductivity of the weld puddle which partially depends on proper shield gas coverage.

APPENDIX A

DATA ACQUISITION SOFTWARE

A.1. MAIN PROGRAM

A.2. MACRO CONTROL PROGRAM

A.1. MAIN PROGRAM

```
C       TITLE: SKY.FOR
C       AUTHOR: HOOMAN HOUSHMAND
C       THIS PROGRAM CONTROLS THE SAMPLING OF AN ANALOG VOLTAGE.
C       THE PROGRAM PROMPTS FOR THE NUMBER OF DATA SETS TO BE ACQUIRED.
C       4096 DATA SAMPLES ARE THEN TAKEN PER DATA SET AND STORED ON
C       A FLOPPY DISK.
C
C       IDATA = DATA BUFFER
C       ISCAN = THE SCAN NUMBER
C       LBLK  = FILE NAME
C
        COMMON /TOT/IDATA(4352)
        INTEGER IDATA,ISCAN
        BYTE LBLK(6)
        INTEGER*2  DBLK(4)
        DATA    IDNAM/2RSY/
        DATA    DBLK(1)/3RSY1/,DBLK(4)/3RDAT/
C
C       TEST THE EQUIPMENT
C
407     TYPE 413
413     FORMAT(' DO YOU WISH TO TAKE A TEST SCAN?'$)
C
        ACCEPT 415,TEST
415     FORMAT(A1)
C
        IF( TEST .EQ. 'Y' ) GO TO 417
        GO TO 419
C
C       TAKE A TEST SCAN
C
417     CALL DMAIT
C
C       ASSUMING ADAC BOARD
C
        DO 409, I5=1,550
C
C       CONVERT THE A/D VALUE TO ITS CORRESPONDING DECIMAL VALUE
C
409     IDATA(I5)=((4095-IDATA(I5))+1)*4.88
C
C       TYPE OUT THE SCAN
C
        DO 411 , I7=0,512,8
411     TYPE *,(IDATA(I7+J7),J7=1,8)
C
        GO TO 400
C
419     TYPE 401
401     FORMAT(' WHAT IS THE SAMPLING FREQUENCY(IN KHz)? '$)
        ACCEPT *,ASF
C
```

```
C
C
C       INQUIRE INTO THE NUMBER OF ITERATIONS
C
C
151     TYPE 155
155     FORMAT(' HOW MANY SCANS ARE TO BE TAKEN?'$)
        TYPE 157
157     FORMAT('  UP TO 50 : '$)
        ACCEPT 156,ISCAN
156     FORMAT(I2)
        IF (ISCAN .GT. 0 .AND. ISCAN .LT. 50 ) GO TO 158
        TYPE 152
152     FORMAT (' INVALID CHARACTER')
        GO TO 151
C
C       ADJUST SCAN# TO REFLECT BLOCKS RATHER THAN SCANS.
C
158     ISCAN=ISCAN*17
C
C
C
C
C       FILE SPECIFICATION FOR STORAGE
C
        TYPE 10
10      FORMAT(' WHAT FILE? ENTER A SIX CHARACTER CODE WORD: '$)
        ACCEPT 20,(LBLK(I),I=1,6)
20      FORMAT(6A1)
C
C
        TYPE 52783
52783   FORMAT(' HIT RETURN TO START DATA AQUSITION '$)
        ACCEPT 415,GO
        TYPE *,(' TAKING DATA')
C
C
C       GET DATA AND INFO ON FLOPPY
C
C
C       RESET BLOCK COUNTER
C
        IBLOCK=0
C
C
        CALL IRAD50(6,LBLK,DBLK(2))
        IF(IFETCH(IDNAM).NE.0) STOP 'FETCH ERROR'
        ICHAN = IGETC()
        IF(ICHAN.LT.0) STOP 'CHANNEL ERROR'
        IF(IENTER(ICHAN,DBLK,0).LE.0) STOP 'ENTER ERROR'
        CALL IPOKE("44,"10100.OR.IPEEK("44))
C
```

```
C       RESET THE DATA BUFFER
C
300     DO 30,I2=1,4352
30      IDATA(I2)=0
C
C       CALL THE MACRO PROGRAM
C
        CALL DMAIT
C
C       GET TIME, DATE, SCAN, AND TOTAL # OF SCAN INFO
C
        CALL INFO(IDATA,ISCAN,IBLOCK)
C
C       GET FREQUENCY RECORDED IN KHz
C
        CALL FREQ(IDATA,ASF)
C
C       WRITE THE DATA ON SYSTEM'S DISKETTE
C
C*****************************************************************
C
C           ''''WRITE ON FLOPPY''''
C
C       LBLK: THE NAME OF FILE ON FLOPPY IN DRIVE ONE.
C             FILE HAS .DAT DESIGNATION
C
C       IDATA: THE INTEGER DATA ARRAY FROM MAIN
C
C       M: DIMENSION OF IDATA
C
C       IBLOCK: THE STARTING BLOCK , COUNT FROM ZERO
CC****************************************************************
C
        IF(IWRITW(4352,IDATA,IBLOCK,ICHAN).LE.0) STOP 'WRITE ERROR'
C
C       ADVANCE BLOCK NUMBERS BY 17 OR 4352 WORDS.
C
        IBLOCK=IBLOCK+17
C
C       CHECK IF THE NUMBER OF SCANS TAKEN (IBLOCK)
C       EQUALS THE NUMBER DESIRED TO BE ACQUIRED (SCAN#)
C
        IF ( IBLOCK .GE. ISCAN ) GO TO 400
        GO TO 300
C
400     CALL CLOSEC(ICHAN)
        CALL IFREEC(ICHAN)
        CALL IPOKE("44,"167677.AND.IPEEK("44))
C
        TYPE 403
403     FORMAT(' DO YOU WISH TO TAKE ANOTHER SCAN?'$)
        ACCEPT 405,ANS
405     FORMAT(A1)
        IF (ANS .EQ. 'Y') GO TO 407
C
        RETURN
        END
```

```
C************************INFO************************************
C
C       GET TIME, DATE, SCAN, AND TOTAL # OF SCAN INFO
C
        SUBROUTINE INFO(IDATA,ISCAN,IBLOCK)
C
        INTEGER IDATA(4352),ISCAN,IBLOCK
C
C       GET TIME IN TICKS PAST MIDNIGHT
C
        CALL GTIM(JTIME)
C
C       CONVERT THE TICKS FOUND INTO HOURS, MINUTES, SECONDS,
C       AND TICKS.
C
        CALL CVTTIM(JTIME,IDATA(4100),IDATA(4101),IDATA(4102),IDATA(4103))
C
C       STORE THREE INTEGER VALUES CORRESPONDING TO THE
C       MONTH, DAY, AND YEAR.
C
        CALL IDATE( IDATA(4105), IDATA(4106), IDATA(4107))
C
C       STORE THE NUMBER OF SCANS
C
        IDATA(4110)=ISCAN/17
C
C       STORE WHAT SCAN
C
        IDATA(4111)=IBLOCK/17
C
        RETURN
        END
C
C*****************************FREQ*********************************
C
        SUBROUTINE FREQ(IDATA,ASF)
C
C       IDATA IS THE DATA ARRAY
C
C       ASF IS THE SAMPLING FREQUENCY
C
        INTEGER IDATA(4352)
C
C
C       TO GET THE KHz PART
C
        IDATA(4120)=IFIX(ASF)
C
C       TO GET THE DECIMAL POINTS
C
        IDATA(4121)=IFIX((ASF-IFIX(ASF))*10000.)
C
        RETURN
        END
```

A.2. MACRO CONTROL PROGRAM

```
        .TITLE HIN5.MAC
        .GLOBL DMAIT
; AUTHOR : HOOMAN HOUSHMAND 20-OCT-83
; THIS SUBROUTINE USES '' ADAC BOARDS '' AT CERL TO TAKE IN
; 4K DATA POINTS
; REFERENCES: i  ADAC INSTRUCTION MANUAL PAGE 59
;             ii INIT.MAC
;
; WAIT UNTIL DMA IS NO LONGER BUSY
;
DMAIT:    TSTB @#DMACSR
          BPL DMAIT
;
; SET 4K POINTS TO BE TAKEN, SPECIFY IN TWO'S COMPLEMENT
;
          MOV #170000,@#DMAWCR
;
; DEFINE THE MEMORY LOCATION
;
          MOV #TOT,@#DMABAR
;
; CLEAR DATA BUFFER FLAG
;
          TST @#ADDBR
;
;
; ENABLE THE DMA
;
          MOV #1,@#DMACSR
;
; SET MULTIPLEXER COMPARISON REGISTER TO ONE CHANNEL OPERATION
;
          MOV #1,@#DMAMCR
;
; SET UNITY GAIN, EXTERNAL ENABLE MODE, ON CHANNEL 0(ZERO) FOR
;     GATE ON A/D
;
          MOV #32,@#ADCSR
;
; WAIT UNTIL DMA PASSES ALL THE POINTS TO THE MEMORY
;
1$:       TSTB  @#DMACSR
          BPL   1$
;
; CLEAR DATA BUFFER FLAG
;
          TST @#ADDBR
;
; DISABLE DMA
;
          MOV #0,@#DMACSR
;
; RETURN TO THE CALLING PROGRAM
;
END1:     RTS  PC
```

```
; DEFINITION OF THE MNEMONICS USED
;
DMAWCR   =   172410     ; DIRECT MEMORY ACCESS WORD COUNT REGISTER
;
DMABAR   =   172412     ; DIRECT MEMORY ACCESS BUS ADDRESS REGISTER
;
DMACSR   =   172414     ; DIRECT MEMORY ACCESS CONTROL STATUS REGISTER
;
DMAMCR   =   172416     ; DIRECT MEMORY ACCESS MULTIPLEX COMPARATOR REGISTER
;
ADCSR    =   177000     ; ANALOG TO DIGITAL CONTROL STATUS REGISTER
;
ADDBR    =   177002     ; ANALOG TO DIGITAL DATA BUFFER REGISTER
;
; MAKE DATA ARRAY , TOT, READ/WRITE , DIRECT , GLOBAL , RELOCATABLE ,
; AND OVERLAYED
;
          .PSECT TOT,RW,D,GBL,REL,OVR
;
; DEFINE IN DECIMAL THE SIZE OF THE DATA ARRAY
;
TOT:      .BLKW  4096.
;
; END OF THE MACRO PROGRAM
;
          .END   DMAIT
```

APPENDIX B

SIGNAL PROCESSING SOFTWARE

B.1. MAIN PROGRAM

B.2. FAST FOURIER TRANSFORM (FFT)

B.3. NORMALIZATION

B.1. MAIN PROGRAM

```
C       THIS PROGRAM PRODUCES AVERAGED POWER SPECTRA
C       AUTHOR HOOMAN HOUSHMAND
c       htst52.FOR
C
        COMPLEX WELD
        VIRTUAL WELD(4096)
        REAL RWELD
        VIRTUAL RWELD(2048)
        INTEGER IWELD(4352)
        BYTE LBLK(6)
C
        TYPE 10
10      FORMAT(' WHAT FILE? TYPE A SIX CHARACTER CODE WORD.')
        ACCEPT 20,(LBLK(I0),I0=1,6)
20      FORMAT(6A1)
C
C       HRED12 IS DISK READ ROUTINE
C
        CALL HRED12(LBLK,IWELD,4352,0)
C
C       READ IN # OF DATUM SETS
C
        ITNOS-IWELD(4110)
C
C
        DO 1 I1=1,2048
1          RWELD(I1)=0
C
        DO 5 I3=1,ITNOS
         IBLOCK=(I3-1)*17
         CALL HRED12(LBLK,IWELD,4096,IBLOCK)
         DO 7 I7=1,4096
7           WELD(I7)=IWELD(I7)
C
C       SET DC TO ZERO
C
         DOUBLE PRECISION STDCZR
         STDCZR=0.0
C
         DO 127 I15=1,4096
127         STDCZR=STDCZR+WELD(I15)
C
         STDCZR=STDCZR/4096.
C
         DO 139 J15=1,4096
139         WELD(J15)=WELD(J15)-STDCZR
C
C       TAKE FFT OF A DATUM SCAN
C
         CALL HFFT(WELD,12)
C
```

```
C       AVERAGE THE POWER SPECTRA
C
        RWELD(0)=1E-14
         DO 3 J2=2,2048
3           RWELD(J2)=RWELD(J2)+(CABS(WELD(J2)))**2
C
5       CONTINUE
C
        DO 121 I9=1,2048
121        RWELD(I9)=RWELD(I9)/ITNOS
C
        IWELD(4111)='AV'
C
        REAL TWELD(2048)
C
        EQUIVALENCE (TWELD(1),IWELD(1))
C
        DO 18683,I=1,2048
18683           TWELD(I)=RWELD(I)
C
C       HSTRNW IS DISK WRITE ROUTINE
C
        CALL HSTRNW(LBLK,IWELD,4352,0)
C
        CALL EXIT
        END
```

B.2. FAST FOURIER TRANSFORM (FFT)

```
C     THIS PROGRAM IS A FFT ROUTINE WITH DOUBLE PRECISION CAPABILITY,
C     IT CAN PERFORM UP TO A 4K POINT FFT.
C     REF: DECIMATION IN FREQUENCY, SKY INTRO MANUAL
C        USE THE SKYMNK ARRAY PROCESSOR
C     AUTHOR HOOMAN HOUSHMAND
      SUBROUTINE HFFT(X,M)
      VIRTUAL X(4096)
      COMPLEX X,U,W,T
      DOUBLE PRECISION PI
      N=2**M
C
C     N IS THE ACTUAL LENGTH OF THE INPUT SEQUENCE
C
      PI=3.14159265358979
C
C     LIMIT THE ITERATIONS TO TWO
C
      DO 20 L=1,2
      LE=2**(M+1-L)
      LE1=LE/2
      U=(1.0,0.0)
      W=CMPLX(DCOS(PI/FLOAT(LE1)),-DSIN(PI/FLOAT(LE1)))
      DO 20 J=1,LE1
      DO 10 I=J,N,LE
      IP=I+LE1
      T=X(I)+X(IP)
      X(IP)=(X(I)-X(IP))*U
10    X(I)=T
20    U=U*W
        INTEGER TEMPL(14,10)
        REAL*4 VIRT(5)
        CALL VINIT(TEMPL,10,VIRT,5)
        VIRT(1)=VIRTUL(X,1,'C','SP')
        CALL VFFT(VIRT(1),1,VIRT(1),1,10)
        VIRT(2)=VIRTUL(X,1025,'C','SP')
        CALL VFFT(VIRT(2),1,VIRT(2),1,10)
        VIRT(3)=VIRTUL(X,2049,'C','SP')
        CALL VFFT(VIRT(3),1,VIRT(3),1,10)
        VIRT(4)=VIRTUL(X,3073,'C','SP')
        CALL VFFT(VIRT(4),1,VIRT(4),1,10)
        CALL VWAIT
        CALL VDONE
      NV2=N/2
      NM1=N-1
      J=1
      DO 30 I=1,NM1
      IF(I.GE.J) GO TO 25
      T=X(J)
      X(J)=X(I)
      X(I)=T
25    K=NV2
26    IF(K.GE.J) GO TO 30
      J=J-K
      K=K/2
      GO TO 26
30    J=J+K
      RETURN
      END
```

B.3. NORMALIZATION

```
C       THIS PROGRAM NORMALIZES THE AVERAGED POWER
C       SPECTRA WITH TOTAL POWER
C       AUTHOR HOOMAN HOUSHMAND
C
        VIRTUAL RWELD(2048)
        REAL RWELD
        INTEGER IWELD(4096)
        EQUIVALENCE (XWELD(1),IWELD(1)),(IWELD(1),YARRAY(1))
        EQUIVALENCE (IWELD(2049),XARRAY(1))
        REAL XWELD(2048)
C
        BYTE LBLK(6)
465     TYPE 10
10      FORMAT(' WHAT FILE? TYPE A SIX CHARACTER CODE WORD.')
        ACCEPT 20,(LBLK(I0),I0=1,6)
20      FORMAT(6A1)
C
        IBLOCK=16
C
C       GET THE AMBIENT INFO
C
C       HTST12 IS DISK READ ROUTINE
C
        CALL HTST12(LBLK,IWELD,256,IBLOCK)
C
C       READ OFF THE SAMPLING FREQUENCY IN KHz
C
        ASF=(IWELD(24)*1.)+(IWELD(25)/10000.)
C
C       CONVERT TO Hz
C
        ASF=ASF*1000.
C
C       READ OFF DATA
C
        CALL HTST12(LBLK,IWELD,4096,0)
C
        DO 1 I1=1,2048
1       RWELD(I1)=XWELD(I1)
C
C       NORMALIZE WITH TOTAL POWER
C
        DOUBLE PRECISION XAVG
C
        XAVG=0
        DO 59 I=1,2048
59      XAVG=XAVG+RWELD(I)
C
        DO 2002 I2002=1,2048
        VALUE=RWELD(I2002)/XAVG
        IF(ABS(VALUE).LT.1.0E-14) VALUE=1.0E-14
2002    RWELD(I2002)=10*ALOG10(VALUE)
C
        GOTO 117
C
```

```
C       ASK OPERATOR WHAT TO DO
C
113     CALL CLEAR
2004    TYPE 101
101     FORMAT(' '/' PRINT PEAKS (P), TYPE PEAKS (T), ZOOM (Z) '/
     X    ' GRAPH SPECTRUM (G), COPY (C), '/
     X    ' SMALL COPY (S), OR JUMP OUT (J)? '$)
C
        ACCEPT 103,IKEY
103     FORMAT(A1)
C
        IF( IKEY.EQ.'P')GOTO 123
        IF( IKEY.EQ.'T')GOTO 125
        IF( IKEY.EQ.'Z')GOTO 90
        IF( IKEY.EQ.'G')COTO 117
        IF( IKEY.EQ.'C')CALL COPY
        IF( IKEY.EQ.'S')CALL SCOPY
        IF( IKEY.EQ.'J')GOTO 109
        GOTO 113
C
C       ASK IF THE OPERATOR WANTS TO DO MORE
C
109     CALL CLEAR
        TYPE 105
105     FORMAT(' '/'  STORE THE MAGNITUDES (S), ANOTHER FILE (F),'
     X   /'  GRAPH SPECTRUM (G), OR END (E)? '$)
C
        ACCEPT 107, LKEY
107     FORMAT(A1)
C
        IF( LKEY.EQ.'G')GOTO 117
        IF( LKEY.EQ.'S')GOTO 111
        IF( LKEY.EQ.'F')GOTO 465
        IF( LKEY.EQ.'E')GOTO 115
        GO TO 109
C
115     CALL EXIT
C
111     TYPE *,(' UNDER DEVELOPMENT')
        GOTO 113
C
C       GRAPH THE SPECTRUM
C
        REAL YARRAY(512)
C
117     DO 121 ,I9=0,511
         YARRAY((I9)+1)=-1.0E15
          DO 119,J9-1,4
           RFFTVA=RWELD(4*(I9)+(J9))
119        IF(YARRAY((I9)+1).LT.RFFTVA)YARRAY((I9)+1)=RFFTVA
121      CONTINUE
C
        CALL MAG(512,YARRAY,FLOAT(0.),FLOAT(ASF/2.))
C
C       INDEXES FROM ZOOM FOR PEAK SEARCH
C
        INIELM=1
        JENDEL=2048
C
        GOTO 113
```

```
C
C       '''''PEAK'''''OPTON
C
C       PRINT OUT THE PEAKS
C
123     CALL TYPE
C
125     TYPE 133
133     FORMAT(' ENTER THE CUTOFF LEVEL: '$)
         ACCEPT*,CUTOFF
C
        TYPE 135
135     FORMAT(//' FREQUENCY',6X,'MAGNITUDE')
C
        TYPE 137
137     FORMAT(' ---------',6X,'---------')
C
        DO 131,I13=INIELM,JENDEL
           IF( RWELD(I13).LT.CUTOFF)GOTO 131
           IF( RWELD((I13)+1).GE.RWELD(I13))GOTO 131
           IF( RWELD((I13)-1).GT.RWELD(I13))GOTO 131
C
             TYPE 129, ((I13)-1)*ASF/4096.RWELD(I13)
129             FORMAT(' ',F8.4,6X,E9.2)
C
131        CONTINUE
C
        CALL NTYPE
C
        TYPE *,(' ')
        GOTO 2004
C
C       ZOOM
C
090     TYPE 100
100     FORMAT(' ENTER THE STARTING FREQUENCY (Hz) : '$)
        ACCEPT *,STFREQ
        IF(STFREQ.LT.(0.0).OR.STFREQ.GT.(ASF/2))GOTO 94
        GOTO 092
94      TYPE*,(' OUT OF RANGE')
        GOTO 090
C
092     TYPE 102
102     FORMAT(' ENTER NUMBER OF POINTS : '$)
        ACCEPT*,NUMPOT
        IF(NUMPOT.LT.2.OR.NUMPOT.GT.512)GOTO 98
        GOTO 96
98      TYPE*,(' OUT OF RANGE')
        GOTO 092
C
C       INITIAL ELEMENT
C
96      INIELM=(4096*STFREQ/ASF)+1
C
C       END ELEMENT
C
        JENDEL=INIELM+NUMPOT-1
C
```

```
C       OVERFLOW PROTECT
C
        IF (JENDEL.GT.2048)JENDEL=2048
C
        NUMPOT=JENDEL-INIELM+1
C
C       PUT DATA IN PLOT BUFFER
C
        DO 104, IZOOMO=INIELM,JENDEL
104     YARRAY(IZOOMO-INIELM+1)=RWELD(IZOOMO)
C
C       FIX THE X ARRAY
C
C       FIND END FREQUENCY
C
        ENDFRQ=(JENDEL-1)*ASF/4096
C
C
        REAL XARRAY(512)
        XINCR=(ENDFRQ-STFREQ)/(NUMPOT-1)
        DO 88,I1=1,NUMPOT
88      XARRAY(I1)=STFREQ+XINCR*(I1-1)
C
        CALL INITGR (5)
        CALL ERASE
        CALL CLEAR
        CALL DPAPER (,5,,,5,5,'GRAY2')
        CALL LNAXIS ('XT','FREQUENCY',,,)
        CALL LNAXIS ('YL','NORMALIZED POWER',,,)
        CALL PDATA (NUMPOT,XARRAY,YARRAY,,,,,,,)
C
        GOTO 113
C
        END
C
C*****************************MAG*****************************
C
        SUBROUTINE MAG(M,YARRAY,BEGIN,END)
        REAL YARRAY(M)
        CALL INITGR(5)
        CALL CLEAR
        CALL ERASE
        CALL DPAPER(,5,,,5,5,'GRAY2')
        CALL LNAXIS('XB','       FREQUENCY Hz',BEGIN,END,.TRUE.)
        CALL LNAXIS('YL','NORMALIZED POWER',,,)
        CALL PDATA(M,,YARRAY,,,,,,,)
        RETURN
        END
```

REFERENCES

[1] M. E. Norris and C. S. Gardner, "Microprocessor controlled weld arc spectrum analyzer," RRL Rep. 412, University of Illinois, Urbana, IL, October 1981.

[2] D. R. Blackmon, V. F. Hock, "An opto-electronic technique for identifying weld defects in real time," Society for Advancement of Material and Process Engineering, pp. 115-124, October 1983.

[3] R. C. Davis and C. S. Gardner, "Spectroscopic analysis of laser welding plasmas," RRL Report 517, University of Illinois, Urbana, IL, July 1982.

[4] H. B. Cary, Modern Welding Technology. New Jersey: Prentice-Hall, 1979.

[5] R. P. Meister, "Weld imperfections: Identification and interpretation," Symposium on Nondestructive Testing of Welds Proceedings, pp. 372-413, 1968.

[6] J. E. Shea and C. S. Gardner, "Spectroscopic measurement of hydrogen contamination in weld arc plasmas," J. Appl. Phys., vol. 54, no. 9, pp. 4928-38, February 1983.

[7] J. Giachino, W. Weeks, G. Johnson, Welding Technology. Chicago, IL: American Technical Society, 1968.

[8] W. H. Wooding, "The inert-gas shielded metal arc welding process," Welding J., vol. 32, April 1953.

[9] Electro-Optics Handbook. Harrison, N. J.: RCA Corp. 1974, pp. 34-43.

[10] J. T. Verdeyen, Laser Electronics. New Jersey: Prentice-Hall, 1981.

[11] J. M. Somerville, The Electric Arc. New York: John Wiley and Sons, Inc., 1959.

[12] W. R. Chynoweth, "A study of the welding arc," University of Illinois, Urbana, IL, May 1947.

[13] "Dolan-Jenner High Temperature Fiber Optics Bulletin 878a," Dolan-Jenner Industries, Inc., Woburn, Mass., 1981.

[14] "HR-320 Instructions Manual," Instruments S. A. Inc., Metuchen, N. J., 1979.

[15] "ADAC Instruction Manuals, "Data Aquisition Systems Compatable with DEC LSI-11, Published by ADAC Corporation.

[16] A. Papoulis, The Fourier Integral and Its Applications. New York: McGraw-Hill, 1962.

[17] C. S. Gardner and J. D. Shelton, "Spatial and temporal filtering technique for processing lidar photocount data," Opt. Lett., vol. 6, no. 4, April 1981.

[18] A. V. Oppenheim and R. W. Schafer, Digital Signal Processing. New Jersey: Prentice-Hall, 1975.

[19] Wavelength and Transition Probabilities for Atoms and Atomic Ions, NSRDS-NBS68, U. S. Government Printing Office, Washington, 1980.

[20] D. W. Peterson and P. L. Ransom, "The calibration and cataloging of spectral emissions from gas metal arc welding of steel from 4100 Å to 7450 Å," RRL Rep. 522, University of Illinois, Urbana, IL, January 1983.

[21] A. Grill, "Effect of current pulses on the temperature distribution and microstructure in TIG tantalum welds," Metallurgical Trans. B., vol. 12B, pp. 187, March 1981.

CUMULATIVE LIST OF RADIO RESEARCH LABORATORY AND
ELECTRO-OPTIC SYSTEMS LABORATORY
REPORTS PREPARED UNDER U. S. ARMY SUPPORT

RRL Rep. No. 512 - M. E. Norris and C. S. Gardner (October 1981), Microprocessor Controlled Weld Arc Spectrum Analyzer.

RRL Rep. No. 517 - R. C. Davis and C. S. Gardner (July 1982), Spectroscopic Analysis of Laser Welding Plasma.

RRL Rep. No. 520 - D. A. Webber and C. S. Gardner (October 1982), Evaluation of a Thermal Imaging Technique for Measuring Welding Travel Speed.

RRL Rep. No. 521 - K. S. Yang and A. H. Schriefer, Jr. (October 1982), A Welding Table Travel Digitization System.

RRL Rep. No. 522 - D. W. Peterson and P. L. Ransom (January 1983), The Calibration and Cataloging of Spectral Emissions from Gas Metal Arc Welding of Steel from 4100Å to 7450Å.

RRL Rep. No. 524 - J. E. Shea and C. S. Gardner (February 1983), Spectroscopic Measurements of Hydrogen Contamination in Weld Arc Plasma.

RRL Rep. No. 525 - D. A. Webber and C. S. Gardner (March 1983), An Image Correlation Technique for Measuring Weld Travel Speed.

EOSL Rep. No. 84-002 - A. Lenef and C. S. Gardner (October 1984), Effects of Optical Emissions From Weld Arcs on the Performance of Welding Robot Vision Systems.

EOSL Rep. No. 84-003 - H. Houshmand and C. S. Gardner (October 1984), Analysis of the Intensity Fluctuations of Optical Emission Lines in Weld Arc Plasmas.

PAPERS PUBLISHED

J. E. Shea and C. S. Gardner, "Spectroscopic measurement of hydrogen contamination in weld arc plasmas," Journal of Applied Physics, 54, 4928-4938, September 1983.